Carbohydrate Polymer Technologies and Applications 8 (2024) 100572

Contents lists available at ScienceDirect

Carbohydrate Polymer Technologies and Applications

journal homepage: www.sciencedirect.com/journal/carbohydrate-polymer-technologies-and-applications

Microwave assisted treatment of carpentry waste wood flour with natural deep eutectic solvents for nanocellulose production and removal of organic pollutants

Giovanni Cisternino [a], Francesca Baldassarre [b,c], Giuseppe Ciccarella [b,c], Piero Mastrorilli [a], Maria Michela Dell'Anna [a,*]

[a] DICATECh, Politecnico di Bari, via Orabona, 4 70125 Bari, Italy
[b] Dipartimento di Scienze e Tecnologie Biologiche e Ambientali, Università del Salento, Via Monteroni s.n.c. 73100 Lecce, Italy
[c] Istituto di Nanotecnologia CNR-Nanotec, Consiglio Nazionale Delle Ricerche, via Monteroni, 73100 Lecce, Italy

ARTICLE INFO

Keywords:
Carpentry waste wood flour
Deep eutectic solvents
Nanocellulose
Water remediation
Organic pollutant

ABSTRACT

Row carpentry waste wood flour, constituted of poplar (~60 %) and fir (~30 %) biomass, was subjected for the first time to microwave-assisted deep eutectic solvent (DES) treatment, with the purposes of solubilizing lignin and hemicellulose, leaving cellulose as solid residue, thus performing a biorefinery. Several acidic (choline chloride/oxalic acid; choline chloride/citric acid; betaine hydrochloride/oxalic acid) and alkaline (urea/choline chloride; glycerol/K_2CO_3) DESs were employed under the same reaction conditions. Since the highest extraction yield was obtained by using choline chloride/oxalic acid DES, the use of the latter was investigated by varying some parameters (temperature, manner of microwave irradiation, addition of water) aiming at increasing the solubilization yield, which in fact in some cases reached satisfying values (60 %) under mild conditions. The solid residues (SRs) recovered after all treatments with all tested DESs were characterized by Thermogravimetric Analysis (TGA), Attenuated Total Reflectance-Fourier Tranform Infrared Spectroscopy, Solid-State NMR Spectroscopy, and titration of surface acid groups. All SRs were also ultrasonicated to produce cellulose nanoparticles which were in turn characterised by transmission electron microscopy (TEM) and dynamic light scattering (DLS) analyses. In addition, the solid residues recovered from acidic DESs were able to decontaminate water from organic pollutants, such as *p*-nitrophenol, by an adsorption process. Thus, the proposed DES treatment efficiently converted carpentry waste wood flour into a valuable biomaterial useful for environmental decontamination.

1. Introduction

Lignocellulosic biomass (LCB) is a promising and alternative material that can be converted into various compounds (Chen et al., 2011; Haldar & Purkait, 2021; Heise et al., 2021; Krasznai et al., 2018; New et al., 2022; Vu et al., 2020), such as biofuels, high-value chemicals, and precious bio-based materials, like nanocellulose (Liu et al., 2021b). LCB has a highly intricate structure in which both cellulosic and hemicellulosic fractions are strongly linked by a plethora of intermolecular hydrogen bonds and are combined between the lignin layers through covalently bound lignin-carbohydrate complexes (LCC), responsible for the well-known LCB recalcitrance (Liu et al., 2017a). For this reason, lignocellulosic biomass needs to be pre-treated for being fractionated into lignin, hemicellulose and cellulose, prior to be converted into chemicals, biofuels or biomaterial (Kumar & Sharma, 2017). Several pre-treatment methods have been developed, including physical, chemical, biological, or a combination of them (Bian et al., 2020;Pradhan et al., 2022). Notably, the pre-treatment process is the most expensive step in lignocellulosic conversion procedure (Chen & Wan, 2018), so the development of cost-effective and environmentally friendly pre-treatment methods for biomass fractionalization is highly desirable. Sustainable chemical pre-treatment approaches, such as acid, alkaline, or enzymatic methods show low efficiency in overcoming the strong bonds of the lignin-carbohydrate complex (Mankar et al., 2022).

Among chemical methods of pre-treatment, the approach comprising the use of ionic liquids (ILs) seems to give promising results (Hou et al., 2017). ILs are a class of solvents that have been gained popularity in recent years due to their unique properties (Mjalli et al., 2014). ILs are

* Corresponding author.
E-mail address: mariamichela.dellanna@poliba.it (M.M. Dell'Anna).

https://doi.org/10.1016/j.carpta.2024.100572

Available online 19 September 2024

composed of organic cations and inorganic or organic anions, and they have a melting point below 100 °C (Sirviö et al., 2016). Compared to traditional solvents, ILs have several advantages, including high solvent capacity for both organic and inorganic materials, negligible vapour pressure, and good chemical and thermal stability (Sirviö et al., 2016). Due to their ability to partially or completely dissolve lignin with high extraction efficiency, ILs have attracted considerable attention in this context (Prado et al., 2013). However, ILs have also some drawbacks. In fact, they are typically synthesized from oil-based chemicals, they are toxic, not biodegradable, moisture sensitive, and expensive (Egorova & Ananikov, 2014). For all these reasons, deep eutectic solvents (DESs) have replaced ILs in many applications (Smith et al., 2014), having the same advantages but not the same drawbacks of ILs. DESs are prepared by mixing two or more components constituted by at least a hydrogen bond donor (HBD) and a hydrogen bond acceptor (HBA) in a specific molar ratio, thus forming multiple hydrogen bonds (Chourasia et al., 2021). Due to the presence of a strong hydrogen bonding network, the resulting melting point of the mixture is lower than that of the original components, preventing them from crystallising. For this reason, DESs have similar properties of ILs, including thermal and chemical stability, high solvent capacity and low vapour pressure (Liu et al., 2021a). Contrarily to ILs, DESs can be made from easily accessible, inexpensive, non-toxic, biodegradable and non-flammable materials such as choline chloride, betaine hydrocloride and organic acids (Sirviö et al., 2016). In addition, DES can be recycled and reused, helping to reduce production costs (Mankar et al., 2022). All those traits make DESs more attractive solvent than ILs (Calvo-Flores & Mingorance-Sánchez, 2021) for biomass pre-treatment (Zhou et al., 2023), extraction of natural products (Nam et al., 2015), synthesis of functional materials (Hayyan et al., 2015), metal processing (Ma et al., 2022), catalysis (Ünlü et al., 2019), cellulose purification (Verdía Barbará et al., 2023) and drug delivery (Zainal-Abidin et al., 2019). Recent studies have shown that DESs are effective in LCB fractionation (Xiao et al., 2024) acting in two ways: by breaking hydrogen bonds between lignin, hemicellulose and cellulose (Tang et al., 2017), and by hydrolysing covalent bonds between lignin and hemicellulose (Ahmed et al., 2023). In addition, DESs have been reported to facilitate the cleavage of C—C and C—O bonds of lignin itself (Ahmed et al., 2023; Ji et al., 2021; Liu et al., 2019; Liu et al., 2017a; Liu et al., 2017b; Sirviö et al., 2016). Many studies regarding LCB pre-treatment with DESs have found beneficial the use of microwave (MW) irradiation (Amoroso et al., 2020; Chen & Wan, 2018; Liu et al., 2017a; Mankar et al., 2022; Shao et al., 2021) instead of conventional heating (Chen & Wan, 2018), due to the MW capability to interact with a dipolar medium, causing strong rotation and vibration of the polarised ions and molecules (Wang et al., 2020b). This property promotes an energy efficient temperature increasing, and rapid heating response in the DES system, with the generation of many hydrogen protons and ions (Duan et al., 2023). The resulting improved polarity in DESs leads to a reduction of the temperature and time of biomass pre-treatment (Isci et al., 2020). The microwave assisted pre-treatment process has shown great promise as it requires less time (Okonkwo et al., 2023) and allows for easier control of the chemical reactions with respect to conventional warming, provides rapid heating, and needs low energy input (Ahmed et al., 2023)'(Cui et al., 2015).

Most works regarding MW-assisted DES treatment of LCB have focused to specific homogeneous biomass substrates (Kohli et al., 2020), such as pine wood (Ceaser et al., 2023; Oh et al., 2020), poplar trees (Liu et al., 2017a; Wu et al., 2014), bamboo (Lin et al., 2020), and others (Amesho et al., 2023), or lignin poor/bleached sources (Duan et al., 2023; Liu et al., 2017b; Hong et al., 2020) aiming in most cases at obtaining cellulose nanofibrils or nanocrystals after mechanical dealing (ultrasonication, ball milling and high-pressure homogenization) (Zhang et al., 2015;'Lee et al., 2018;'Xie et al., 2016). The reason for focusing on a specific lignocellulosic substrate is intuitive, being biopolymer structures dramatically dependent on their source (Zhang & Naebe, 2021). Therefore, the successful of any biorefinery process also depends on LCB source (Abolore et al., 2024). Few investigations have been devoted to DES-treatment of heterogeneous LCB wastes, such as housing wastes (Abbasi et al., 2024). Indeed, to the best of our knowledge no biorefinery studies employing DESs have been focused on carpentry waste wood flour (CWWF), which is a heterogeneous and not easily fractionable lignocellulosic source. Recently, in our research group preliminary work has been devoted to CWWF, which has been treated with an acidic natural DES (NADES) constituted of choline chloride and oxalic acid in a 1:1 molar ratio, under microwave irradiation (Colella et al., 2022). Following our studies on CWWF valorisation by DESs, in the present work many DESs combinations (acidic and basic) and many different reaction conditions were investigated aiming at converting waste wood flour into eco-friendly materials with higher added value. The objectives of the present study were focused in developing the best conditions for obtaining from CWWF two different valuable products: 1) lignin-rich nanocellulose; 2) a biomaterial useful in environmental field for water decontamination from organic pollutants. In fact, many cellulose-based biomaterials have gained importance for water decontamination purposes (Esposito et al., 2021; Landge et al., 2022; Li et al., 2023; Lombardo & Thielemans, 2019; Mahfoudhi & Boufi, 2017; Patel et al., 2019; Wang, 2019), due to the hydrophilic properties of cellulose itself. Even pure cellulose treated with DES has been found effective for removing an organic compound such as methylene blue from water (Cao et al., 2022). Therefore, potentially CWWF which contains a large amount of cellulose, once treated with DES, could act as an interesting biomaterial useful for environmental decontamination objectives. In addition, the advantage of using CWWF instead of pure cellulose raises from the consideration that CWWF includes also lignin, which could positively affect the absorption capability towards organic compounds due to its hydrophobic features. For the present work, CWWF was composed mostly of poplar (70 % *c.a.*) and fir (30 % *c.a.*) wood. Although most recent works have been aimed at yielding pure (nano and/or micro) cellulose from biomass, the eventual retention of a small amount of lignin in the final product has been reported not to be a drawback (Liu et al., 2020; Liu et al., 2024; Rojo et al., 2015). In fact, in principle the presence of lignin in the residue obtained from DES treatment of CWWF could enhance its capability of retention of organic molecules due to aromatic hydrophobic interactions, thus increasing its performances as water decontaminator from organic pollutants (Coletti et al., 2013; Esposito et al., 2021; Landge et al., 2022; Li et al., 2023; Lombardo & Thielemans, 2019; Mahfoudhi & Boufi, 2017; Patel et al., 2019; Wang, 2019; Yaneva et al., 2013; Zhou et al., 2014). Moreover, nanocellulose containing lignin has been proven to bear interesting features in the field of food packaging (Wang et al., 2024), coating materials (Liu et al., 2023), and agriculture applications (Channab et al., 2024; Baldassarre et al., 2023).

Although the microwave assisted treatment method of CWWF proposed in the present paper had some drawbacks for nanocellulose production due to the poor yields in isolated nanoparticles, however, it turned to be very efficient for converting lignocellulosic waste biomass into a valuable biomaterial for water decontamination from organic pollutants.

2. Materials and methods

2.1. Materials and chemicals

Carpentry waste wood flour (CWWF) was provided by a local carpenter. CWWF was composed mostly of poplar (70 % *c.a.*) and fir (30 % *c.a.*) wood. The chemical reagents employed in this work were: choline chloride (99 %, Acros Organics); oxalic acid dihydrate (99 %, Scharlab); urea (98 %, Alfa Aesar); glycerol (99 %, Acros Organics); potassium carbonate (99 %, Alfa Aesar); betaine hydrochloride (99 %, Alfa Aesar); anhydrous citric acid (99 %, Honeywell), cellulose (Randacell 150, Spagro s.r.l.), lignin (Sigma-Aldrich), 4-nitrophenol (for synthesis, Merck). All the water utilized was purified by Adrona Crystal double deionization system.

2.2. NADESs preparation

The synthesis procedure of the various NADES mixtures employed in the present work is almost the same for all of them with slight modifications. The specific procedures are described below (temperature SD = ± 0.5 °C):

- The choline chloride (ChCl)/oxalic acid (OA) NADES was prepared by continuously mixing the two components in a 1:1 molar ratio and heating at 80 °C until a transparent liquid was obtained and almost all the water evaporated (this water was naturally present in both ChCl and OA). For the 10 % and 20 % water mixtures, the correct amount of water was weighed and added to the clear NADES mixture (Ma et al., 2019);
- The urea/ChCl NADES was prepared by continuously mixing the two components in a 2:1 molar ratio and heating at 80 °C until a transparent liquid was obtained and almost all the water evaporated (Sirviö et al., 2015);
- The K_2CO_3/glycerol DES was prepared by continuously mixing the two components in a molar ratio of 1:7 and heating at 80 °C until a transparent liquid was obtained and almost all the water evaporated (Gan et al., 2020);
- The ChCl/citric acid (CA) NADES was prepared by mixing the two components at 80 °C in a molar ratio of 1:1 and immediately adding the proper amount of water to reach 16.7 % water in the mixture (10 g of water for 50 g of NADES). In this case the water addition was mandatory, otherwise the NADES would be too viscous and not transparent.
- The betaine hydrochloride/OA NADES (Siani et al., 2020) was prepared by mixing the two components in a molar ratio of 1:2 and heating at 80 °C until a transparent liquid was obtained and almost all the water evaporated.

2.3. Microwave assisted biomass treatment

The biomass treatment was carried out by mixing 5 g (or 2.5 g for the betaine hydrochloride/OA NADES and the K_2CO_3/glycerol DES) of 80 Mesh (177 μm diameter size) sieved CWWF with 50 g of freshly prepared NADES. The mixture was then stirred until all the biomass was in contact with the NADES. Afterwards, the mixture was placed in the microwave reactor (Ethos E, Milestone). The reaction was carried out at 80 °C for 1 hour in an open system (temperature SD = ± 0.5 °C). The maximum power of the microwave reactor was set at 500 W (SD = ± 5 W) and the microwave irradiation was discontinuous, so that the temperature of the system remained constant during the reaction. Under the same conditions, the reaction with ChCl/OA was also carried out at 90 °C. After 1 h, the reaction mixture was then cooled by the ventilation system of the microwave reactor and 100 mL of a 1:1 water/acetone solution was added. Afterwards, the reaction mixture was vacuum filtered, and the obtained solid residue (SR) was washed with deionized water (3 x 10 mL) and then stored wet in a refrigerator at 4 °C with the addition of a few drops of chloroform to prevent the formation of mould (Martelli-Tosi et al., 2018).

ChCl/OA DES reaction was carried out also under ultrafast (UF) microwave conditions, maintaining steady the power (continuous irradiation) and stopping the MW irradiation once reached the target temperature. This fast reaction took place in short times (45–70 s), thanks to the synergism between the DES and the microwaves under continuous irradiation (Chen & Wan, 2018). The conditions used are detailed below:

- Reaction UF1: performed in a closed vessel at 250 W with continuous irradiation. The total sample (DES and CWWF, 20 g) reached 156 °C in 60 s.
- Reaction UF2: performed in a closed vessel at 200 W with continuous irradiation. The sample (DES and CWWF, 20 g) reached 103 °C in 45 s.
- Reaction UF3: performed in a closed vessel at 150 W with continuous irradiation. The sample (DES and CWWF, 20 g) reached 82 °C in 75 s.

2.4. Nanocellulose synthesis and process yield

Nanocellulose suspensions were prepared from the residual solids recovered from DES after treatment. Specifically, a certain amount of wet residual solid (0.5 g) was weighed into a flask and added of distilled water (50 mL). The solid residue was kept wet to enhance nanocellulose yield. The resulting heterogeneous mixture was then ultrasonicated at the maximum power available for the ultrasonic bath used in the present work (Sonorex Super 10 P, Bandelin), *i.e.* 430 W and 35 kHz frequency for 20 min at 25 °C. Moreover, some final tests were performed with a probe ultrasonicator, namely Vibracell VCX750 (Sonics, USA). For the latter, the ultrasonic frequency was set at 20 kHz, the processing time was 25 min, the amplitude automatically reached 5 % and the pulse (4 s on and 2 s off) was activated. The mean temperature (25 °C) was kept steady by using a cooling jacket which avoided temperature increasing during ultrasonication process. The mixture was then centrifuged at 2200 rpm (SD = ± 0.5 rpm) for 12 min to separate the solid residue from the nanocellulose suspension, which was in turn stored in a refrigerator at 4 °C with the addition of few drops of chloroform to prevent the formation of mould (Martelli-Tosi et al., 2018).

A small portion of the nanocellulose suspension was used for the calculation of the dimensional reduction yield operated by the ultrasonication process. In details, a certain amount of the suspension was dried at 90 °C to constant weight in an oven. The yield was calculated according to the Eq. (1) (Wang et al., 2021):

$$Y_{NC}^{\%} = \frac{W_{B+NC,d} - W_B}{W_{SR,w} * M_{SR}} * \frac{V_{SR}}{V_{NC}} * 100 \quad (1)$$

Where $W_{B+NC,d}$ is the weight of the beaker containing the dried nanocellulose, W_B is the weight of the beaker, $W_{SR,w}$ is the weight of the total amount of wet solid residue (SR) submitted to ultrasonication, M_{SR} is a number (<1) accounting for the moisture content in the total amount of wet SR submitted to ultrasonication ($M_{SR} \approx 0.80$), V_{SR} is the total volume of the initial ultrasonicated suspension and V_{NC} is the small portion of the volume submitted to the drying process.

2.5. TGA/DTG analysis

The thermal stability of the SRs was assessed using a termogravimetric analyser (Pyris 6 TGA, Perkin Elmer). An average amount of 20 mg of samples were heated at 10 °C/min from 30 °C to 700 °C under 50 mL/min N_2 flow.

2.6. FTIR-ATR analyses

IR analyses were performed with an attenuated total reflectance Fourier transform infrared spectrometer (FT/IR-4200, Jasco) operating in the 550 cm^{-1} to 4000 cm^{-1} range using a ZnSe crystal. The spectra were recorded with an accumulation of 32 scans at 4 cm^{-1} resolution.

2.7. Carboxyl groups content quantification

Carboxyl groups were quantified by acid-base titration according to the method described by Barbash et al. (2022). Briefly, 0.5 g of dry SR was treated with 0.01 M HCl for 1 h to acidify all proton-accepting sites and then washed with distilled water to remove residual acid. The resulting solid was suspended for 2 h in 80 mL calcium acetate solution obtained by diluting with water 30 mL of 0.25 M calcium acetate solution (up to 80 mL). During this period, the carboxylic acid functionalities anchored to the surface of the solid transferred their protons to the acetate, forming acetic acid. The advantage of using calcium acetate instead of a more usual sodium or potassium acetate, was due to the higher capability of calcium cations to exchange with protons with respect to sodium or potassium ions. Afterwards, the suspension was centrifuged, and 25 mL of the supernatant water phase was taken off and titrated with 0.01 M NaOH using phenolphthalein as indicator. The carboxyl groups content was calculated as it follows (Eq. (2)):

$$CGC\left[\frac{mmol}{g}\right] = \frac{\frac{80}{25} * 0.01 * V_{NaOH}}{W_{SR,dry}} \tag{2}$$

where CGC is the carboxyl groups content, V_{NaOH} is the volume (in mL) of NaOH solution used in the titration and $W_{SR,dry}$ is the weight (in g) of the solid residue subjected to carboxyl quantification.

2.8. ^{13}C solid-state NMR spectroscopy (SSNMR)

^{13}C SSNMR experiments were performed on a Bruker Avance I 400 spectrometer (^{13}C, 100.6 MHz) using a 4.0 mm HX MAS probe at room temperature. Samples were packed in zirconia rotors. A two-pulse phase-modulation (TPPM) decoupling scheme was used for the ^{1}H-decoupling. ^{1}H$-^{13}$C CP/ MAS NMR experiments were performed using a contact time of 1.0 ms, a recycle delay of 4 s, a MAS rate of 9 kHz, and an acquisition time of 42 ms. 1024 transients were acquired for the ^{13}C NMR spectrum of each solid residue, in a spectral region of 240 ppm and with 2048 acquired point per sample. The crystallinity index (CrI) of cellulose was calculated by dividing the area of the C4 crystalline peak (integrating the peak from 87 to 92 ppm) by the total area (crystalline and amorphous) assigned to the C4 peaks (integrating the region from 80 to 92 ppm)(Colella et al., 2022).

2.9. Dynamic light scattering (DLS) analysis

Cellulose derived nano-colloids stability and size distribution were investigated by average hydrodynamic diameter, polydispersity index and ζ-potential measurements through Dynamic Light Scattering (DLS). Samples were analysed with a Nano ZS90 (Malvern Instruments, UK) instrument. The ζ-potential analysis was carried out by Laser Doppler Velocimetry (LDV). Measurements were performed at 25 °C, in filtered distilled water (0.45 μm), at the refractive index of cellulose (1.469). The ζ-potential values are reported as the mean of 5 measurements; each of them derived from 20 different runs to establish measurement repeatability. Particle size distribution data are reported as the mean of three measurements each of them derived from 14 different runs to warrant repeatability.

2.10. TEM analyses

The morphology of cellulose derived colloids was analysed by transmission electron microscopy (TEM). A drop of each water suspended sample (10 μl) was placed on a standard carbon coated 200-mesh copper grid and left at RT. The TEM micrographs were acquired analysing the grid under a JEOL JEM 1400Plus microscope with LaB6 source, at an accelerating voltage of 80 kV.

2.11. 4-nitrophenol adsorption setup and UV–Visible spectrophotometry

For each experiment, 20 ml of 20 ppm 4-nitrophenol (4-NP) solution was exposed to 0.5 g of biomass solid residue (SR) for 50 min at 25 °C. A first estimation of the adsorption capacity of the synthesised materials for 4-nitrophenol was carried out by UV–visible spectrophotometry (Jasco V-670 spectrophotometer). The working range was between 250 nm and 500 nm and the experimental pH was <3, thus suitable for the existence of the phenolic form. The choice to operate in an acidic environment was dictated by the lower value of the molar absorption coefficient of 4-NP compared to its phenolate. Detecting 4-NP instead of its anion avoided long dilution series, being very high the response of the used instrument.

3. Results and discussion

3.1. Reaction performances and solid residue characterization

Carpentry waste wood flour (CWWF) was treated with several DES mixtures (acidic or alkaline, see Scheme 1) under MW irradiation (Fig. 1) and the reaction outputs were evaluated. It has been reported that choline chloride (ChCl)-oxalic acid (OA) (1:1) mixture is the most suitable DES for obtaining high yields in nanocellulose starting from specific LCB sources (such as buckwheat chaff, bagasse, cotton pulp, poplar tree, and so on) (Amesho et al., 2023). However, due to the high heterogeneity of CWWF, it deemed worth testing the performance of several DES combinations, aiming at obtaining solid residues still containing a certain amount of lignin. Indeed, the following DES mixtures were tested for CWWF processing: ChCl-OA (1:1) (acidic); ChCl/ (citric acid) CA (1:1) (acidic); betaine hydrochloride/OA (1:2) (acidic); urea/ChCl (2:1) (alkaline); glycerol/K_2CO_3 (7:1) (alkaline). Moreover, the addition of 10 % and 20 % H_2O to the ChCl-OA (1:1) DES was also investigated, due to well-known beneficial effects of water on fluidity parameters and temperature homogeneity (Ma et al., 2019).

The reaction conditions used for the individual mixtures and their performances in terms of weight loss of the starting CWWF (yield of solubilization) are summarised in Table 1.

The $Y\%_{solubilization}$ is the weight loss percentage of the solid biomass after the reaction, mainly due to the decomposition of cellulose and hemicellulose into simpler saccharides and partial dissolution of lignin. The $Y\%_{solubilization}$ was calculated as follows (Eq. (3)):

$$Y^{\%}_{solublization} = \left(1 - \frac{W_{SR}}{W_{CWWF}}\right) * 100 \tag{3}$$

where W_{SR} is the weight of the solid residue after reaction and W_{CWWF} is the weight of the initial lignocellulosic biomass. All DESs considered belonged to NADESs category, except for the K_2CO_3/glycerol mixture. It is worldwide accepted that DESs should ensure good dissolution of lignin, hemicellulose, amorphous cellulose, and all their oligomers and/ or monomers, while leaving the crystalline cellulose as insoluble solid. The mechanism of action of DESs has been studied and thought to be very much dependant on the starting substrate (Liu et al., 2017a). The very strong hydrogen bonds of lignin-carbohydrate complexes in biomass should be weakened because of the formation of competing hydrogen bonds between the carbohydrates/lignin hydroxyl groups and chloride ions/hydroxyl groups from DESs. This causes the loosening of the plant cell wall. Moreover, the H^+, derived from the DESs' donor, may catalyse the selective cleavage of ether or ester bond (hydrolysis) triggering hemicellulose removal and delignification. At the end, the surface of the solid residue might be modified by the esterification of the hydroxyl groups of cellulose with acidic DESs containing carboxylic moieties, which can facilitate the production of nanocellulose (Liu et al., 2021a). For all these reasons, generally the greater the weight loss of biomass the higher the DES activity in terms of biorefinery agent. Table 1 shows that acidic DESs (entries 1–3) gave higher yields of solubilization (yields ranging from 25 to 35 %) with respect to alkaline DES (entries 4–5, yields = 15–22 %) in 1 h at 80 °C under MW continuous irradiation. This occurrence might be explained by considering that under MW irradiation, acidic DESs produce a huge amount of proton ions able to destroy both hydrogen and ester/ether bonds in lignocellulosic biomass. In addition, among acidic DESs the most performant was the ChCl/OA (1:1) mixture (entry 1), as already reported for other lignocellulosic starting materials (Yu et al., 2019). Apparently, betaine hydrochloride/OA (1:2) DES (entry 3) had the same activity of ChCl/OA (1:1) blend under the same reaction conditions (entry 1). However, the

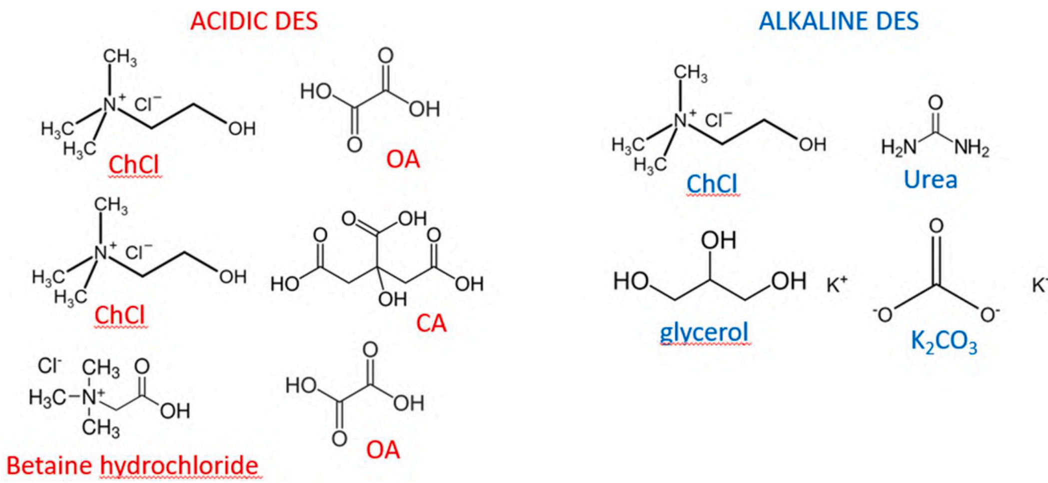

Scheme 1. DES mixtures used for the treatment of CWWF.

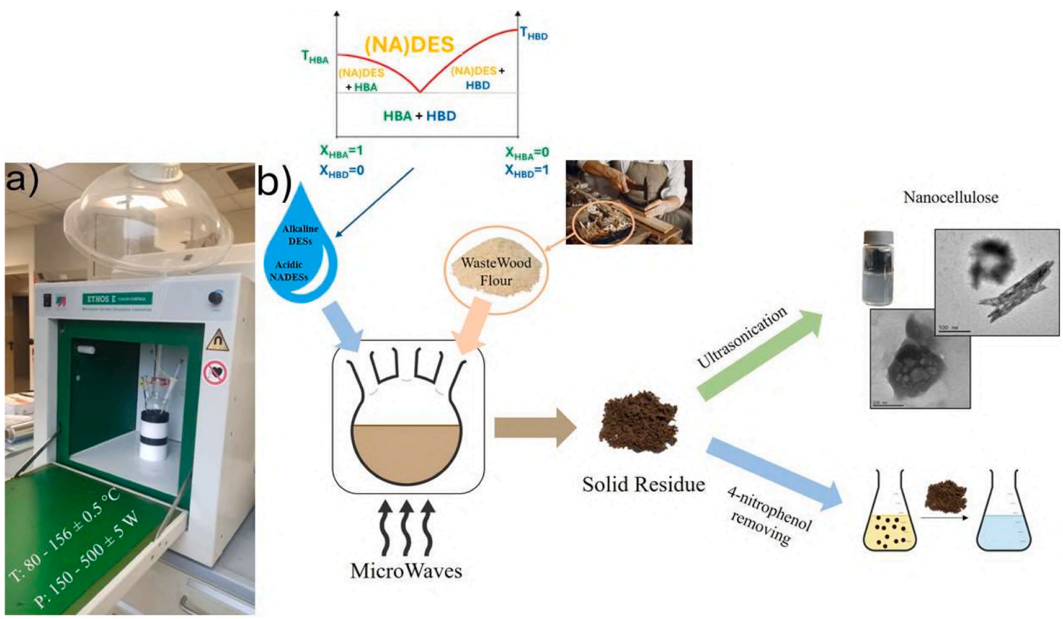

Fig. 1. a) MW equipment and b) **s**equential steps of MW-assisted treatment of CWWF with DES.

amount of CWWF used for betaine hydrochloride/OA (entry 3) was half than the quantity employed for ChCl/OA (entry 1), due to the high viscosity of betaine hydrochloride/OA mixture that hampered the proper mixing of the biomass with the DES solvent. For this reason, the subsequent tests reported in Table 1 (entries 6–11) were carried out only in the ChCl/OA DES. By increasing the temperature up to 90 °C in the ChCl/OA DES system (entry 6), the solubilization yield became almost double (57 %) with respect to the same treatment carried out at 80 °C ($Y\%_{solubilization}$ = 33 %, entry 1). Similar results ($Y\%_{solubilization}$ = 60 %, entry 7) were obtained by performing the ChCl/OA DES treatment under ultrafast conditions UF1, by keeping steady the power (250 W) until temperature reached 156 °C (t= 60′′) (Chen & Wan, 2018). The other ultrafast conditions tested (entries 8 and 9) resulted in almost the same solubilization yields obtained in the traditional microwave assisted reaction (entry 1) with the advantage of taking 45′′ or 75′′ treatment time instead of 1 h reaction time. The addition of certain amount of water to the ChCl/OA DES mixture was also studied (entries 10 and 11), being water able of enhancing microwave irradiation effects and improving DES mixture fluidity parameters (Ma et al., 2019). The addition of 10 % H_2O slightly increased the solubilization yield (40 %, entry 10) with respect to the same system without added water ($Y\%_{solubilization}$ = 33 %, entry 1). However, a 20 % H_2O addition did not bring any advantage to the solubilization yield (33 %, entry 11).

All the residual solids (SRs) obtained after the treatments reported in Table 1 were subjected to thermogravimetric, IR, NMR analyses and carboxylic group titration aiming at evaluating the possible differences caused by the different DESs or conditions used.

3.1.1. Thermogravimetric analyses

Thermogravimetric analysis (TGA) is useful for estimating the chemical composition of the lignocellulosic biomass (Caputo et al., 2021), and on the base of TGA curve the percent amounts of cellulose, hemicellulose and lignin in the starting CWWF were roughly 50 %, 30 % and 20 %, respectively (Fig. 1). All SRs coming from the treatments described in Table 1 were also subjected to TGA analyses. In the following, for the sake of clarity, TGA graphics were grouped in Figs. 2-4. Fig. 2 reports TGA and derivative thermogravimetric curves of either the starting CWWF and all SRs obtained after treatment with NADESs under MW discontinuous irradiation for 1 hour (SRs corresponding to entries 1–6 of Table 1), using cellulose and lignin as

Table 1
Reaction conditions for each DES mixture and yield of solubilization of the starting CWWF.

Entry	DES Mixtures	CWWF/DES mass Ratio	MW-assisted reaction conditions[a]	Yield (%) solubilization
1	ChCl/OA (1:1)	1:10	1 h, 80 °C	33
2	ChCl/CA (1:1)	1:10	1 h, 80 °C	25
3	Betaine hydr. /OA (1:2)	1:20	1 h, 80 °C	35
4	Urea/ChCl (2:1)	1:10	1 h, 80 °C	15
5	Glycerol/K_2CO_3 (7:1)	1:20	1 h, 80 °C	22
6	ChCl/OA (1:1)	1:10	1 h, 90 °C	57
7	ChCl/OA **UF1**	1:10	156 °C peak reached in 60 s	60
8	ChCl/OA **UF2**	1:10	103 °C peak reached in 45 s	37
9	ChCl/OA **UF3**	1:10	82 °C peak reached in 75 s	30
10	ChCl/OA (1:1) + 10 % H_2O	1:10	1 h, 80 °C	40
11	ChCl/OA (1:1) + 20 % H_2O	1:10	1 h, 80 °C	33

[a] SD = ± 0.5 °C for reported temperature values.

references. All the TGA curves reported an initial water loss in the range of 40 - 120 °C (Fig. 2a and 2c). Although solubilization yield values (Table 1) revealed that the highest solubilization amount was reached with the ChCl/OA mixture at 90 °C or under UF1 conditions, TGA analysis showed that ChCl/CA treatment was the most selective towards cellulose, giving the best results in terms of loss amount of hemicellulose and lignin. In fact, TGA curve of SR treated with ChCl/CA DES reported the highest content in cellulose among all solid analysed (Fig. 2a and 2b). On the other hand, the only DES without chloride anion used, *i.e.* the glycerol/K_2CO_3 mixture, gave opposite results. The glycerol/K_2CO_3 mixture seemed to better solubilize (presumably amorphous) cellulose rather than lignin. In fact, glycerol/K_2CO_3 treated SR showed an enhanced content of lignin with respect to pristine CWWF (Fig. 2a and 2b). However, all other considered DES mixtures gave SRs similar in composition to the starting wood flour (Fig. 2a and 2b). Another interesting consideration could be put forward for TGA curves of SRs treated with ChCl/OA at different temperatures for 1 h. In fact, a close inspection of TGA graphs in the range temperature from 500 °C to 700 °C (Fig. 2b) reveals that lignin fraction in the residual solids slightly increases as the treatment temperature increases, probably due to the depolymerization of the amorphous cellulose (Ji et al., 2021). Moreover, DTG graph (Fig. 2c) shows a sharp decomposition peak at 370 °C for all SRs, except for the residue treated with glycerol/K_2CO_3 mixture (decomposition DT = 335 °C), being decomposition DT of CWWF located at 360 °C.

Fig. 3 reports thermogravimetric and derivative thermogravimetric curves of SRs obtained from ChCl/OA mixture under ultrafast conditions (corresponding to entries 7–9 of Table 1). Fig. 3b highlights an obvious temperature effect due to the partial depolymerisation of cellulose, as previously mentioned. In fact, UF1 performed at the highest temperature of 156 °C (corresponding to entry 7 of Table 1) gave a SR richer in lignin than UF2 and UF3 SRs (belonging to entries 8 and 9 of Table 1, respectively), being the latter in turn similar in composition to SR obtained with conventional MW assisted treatment. In addition, TGA curve of SR obtained in 60″ under UF1 conditions is comparable to that reported for SR subjected to conventional MW assisted treatment at 90° for 1 h (see Fig. 2b). All these information suggested that the ultrafast (UF) treatments, though very short time taking, modified the characteristics

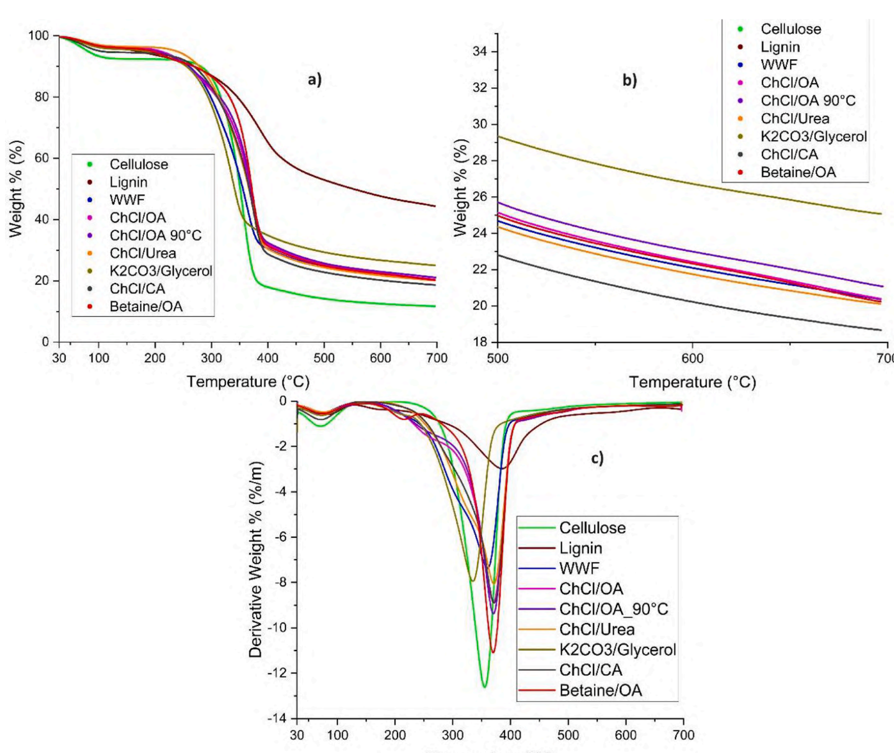

Fig. 2. a) thermogravimetric curves of cellulose, lignin and SRs obtained from different NADES mixtures; b) expansion of Fig. 2a in the 500–700 °C T range; c) derivative thermogravimetric curves.

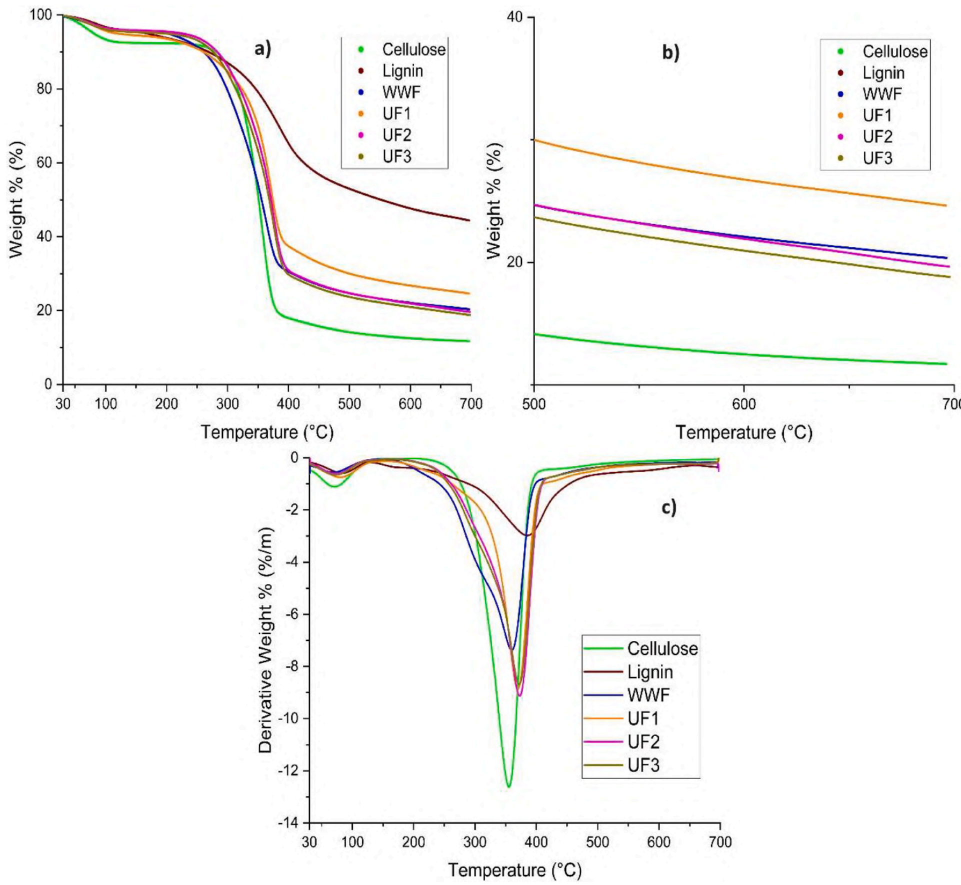

Fig. 3. a) thermogravimetric curves of cellulose, lignin and SRs obtained from different ultrafast reactions (UF1, UF2, UF3); b) expansion of Fig. 3a in the 500–700 °C T range; c) derivative thermogravimetric curves.

of the treated CWWF in the same manner of the corresponding traditional microwave action, pointing out that similar results can be achieved in a shorter time and at a lower cost.

Fig. 4 shows thermogravimetric and derivative thermogravimetric curves of SRs obtained from ChCl/OA mixture without and with the addition of 10 % H_2O (5 g of H_2O and 45 g of NADES) and 20 % H_2O (10 g of H_2O and 40 g of NADES). By comparing these curves to each other (Fig. 4b), no relevant changes could be detected after water addition to the system. This is an important statement, because as already mentioned, water addition reduces both the viscosity of the medium and the overall process cost and can improve homogeneity and flow parameters in an industrial reactor (Ma et al., 2019).

3.1.2. FT-IR analyses

The starting lignocellulosic biomass and all SRs obtained by the treatments summarized in Table 1 were also characterized by IR spectroscopy, taking cellulose and lignin as references. Fig. 5 reports the FT-IR spectra of lignin, cellulose and the starting material (carpentry WWF). In all of them, the broad band extending from 3600 to 3000 cm^{-1} attributed to –OH stretching (in lignin, cellulose and hemicellulose) and the weak broad peak at 2900 cm^{-1} belonging to –CH stretching vibration in methyl and methylene groups (Boeriu et al., 2004) are visible. Carpentry WWF IR spectrum (blu line of Fig. 5) shows fingerprint peaks of cellulose and hemicellulose, which covered most of the lignin characteristic bands, being lignin in lesser amount (30 % *ca*) with respect to cellulose and hemicellulose in wood lignocellulosic biomass. Among them, the peak at 1640 cm^{-1} and the very intense band at 1027 cm^{-1} belonging to bending vibration mode of the absorbed water (Coletti et al., 2013) and to the asymmetric stretching of C—O—C glycosidic bond (Colella et al., 2022) of cellulose and hemicellulose overlap to the characteristic adsorption peaks of the different kinds of lignin (Boeriu et al., 2004).

Fig. 6 shows the FT-IR spectra of the starting carpentry WWF and the SRs obtained with the microwave assisted different DES treatments reported in entries 1–6 of Table 1. The use of carboxylic acids in DES mixture can promote the esterification of cellulose of the starting lignocellulosic biomass (Liu et al., 2021a). If esterification occurred, an increased intensity of the peaks belonging to C = O carboxyl (1720 cm^{-1} *ca*) and C—O ester group (1200 cm^{-1} *ca*) stretching vibration modes should be visible in IR spectra of the treated solids with respect to the starting biomass.

Fig. 6 shows that after MW-assisted DES treatment an increasing in the intensity of the peaks at 1720 cm^{-1} and 1200 cm^{-1} was generally detected. However, this occurrence could not be always ascribable to esterification process. In fact, in the case of SR coming from betaine/OA treatment the reduction of the amount of hemicellulose and amorphous cellulose detected by the analyses discussed in the previous paragraphs could have enhanced the intensity of the band at 1270 cm^{-1} *ca* belonging to G unit of lignin (Wu et al., 2014).

By comparing IR spectra of SRs obtained after the MW treatment with ChCl/OA DES with and without the addition of 10 % and 20 % of H_2O, no significative differences could be detected between them in the regions at 1720 cm^{-1} and 1200 cm^{-1} (Fig. 7), confirming that the addition of water could be beneficial for an economical point of view.

Fig. 8 reports FT-IR spectra of SRs obtained after treatment with ChCl/OA DES under ultrafast microwave conditions (UF1, UF2 and UF3). The IR spectrum of SR coming from UF1 (treated at 156 °C) resembles that of SR obtained by ChCl/OA DES reacted at 90 °C for 1 h, showing a decreasing of the relative intensity of the characteristic peaks of cellulose and hemicellulose with respect to those of lignin, thus

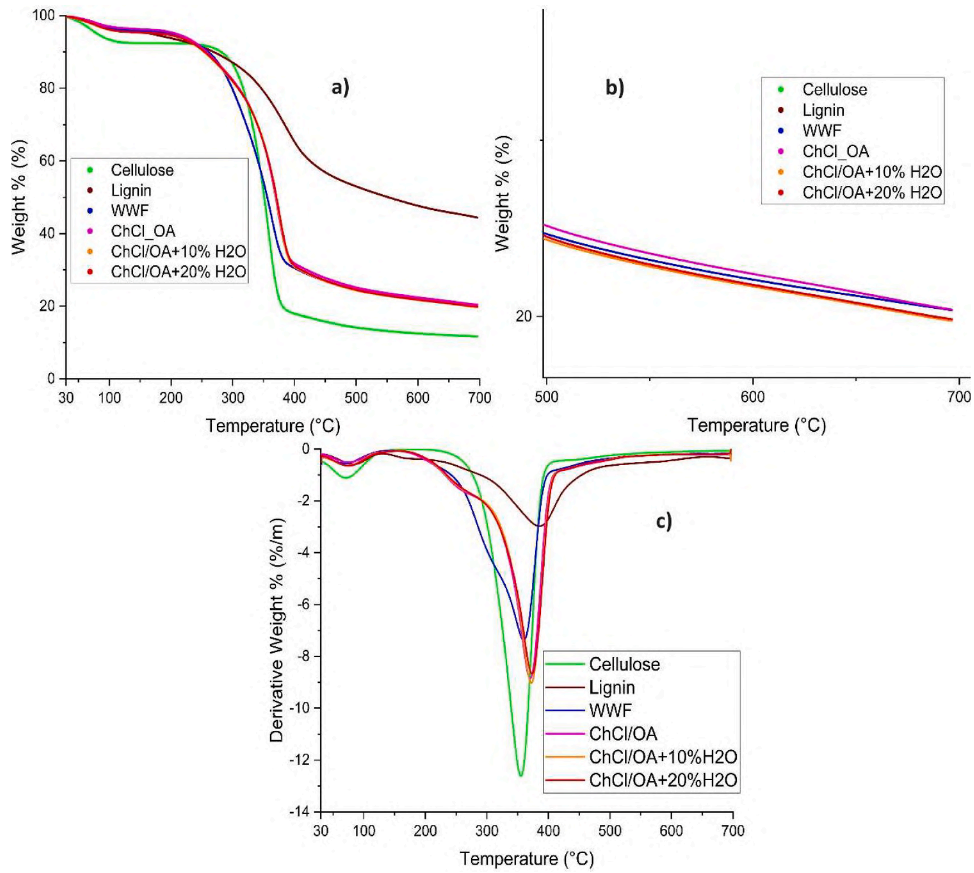

Fig. 4. a) thermogravimetric curves of cellulose, lignine and SRs obtained from ChCl/OA, ChCl/OA+ 10 % H_2O and ChCl/OA+ 20 % H_2O; b) expansion of Fig. 4a in the 500–700 °C T range; c) derivative thermogravimetric curves.

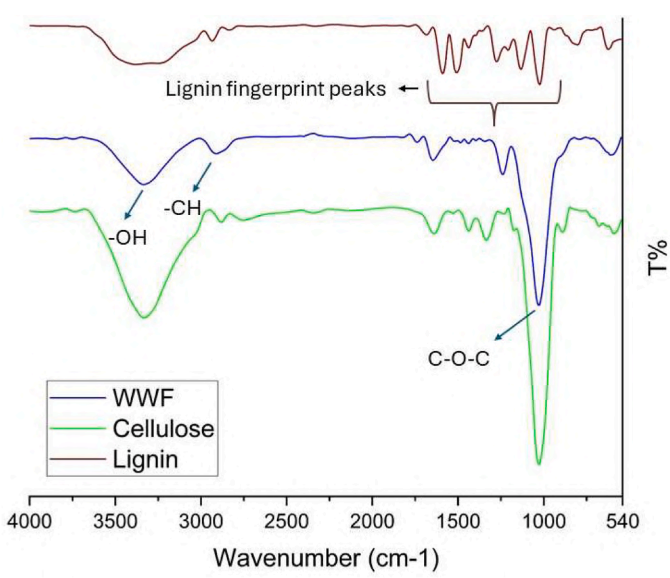

Fig. 5. FT-IR spectra of carpentry WWF, cellulose and lignin.

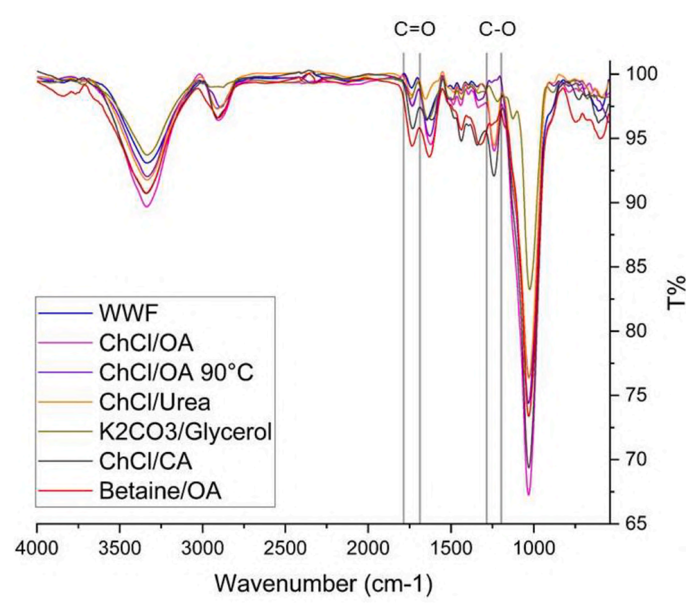

Fig. 6. FT-IR spectra of the different SRs compared to the starting wood waste flour (WWF). The vertical grey lines mark the peaks due to esterification.

confirming the results obtained by TGA analyses, which suggested depolymerization of hemicellulose and amorphous cellulose. Moreover, IR bands reported in Fig. 8 suggests that SR of UF3 treatment in ChCl/OA DES had the highest content of cellulose and the highest degree of esterification among SRs obtained from UF1, UF2 and UF3 (see grey lines of Fig. 8).

3.1.3. *Carboxylic group content (CGC) assessment*

The possible esterification of DES containing carboxylic acids with cellulose -OH groups could be detected by IR analyses (Liu et al., 2021a), as discussed in the previous paragraph. However, the IR peaks assignment belonging to the resulting ester moieties is certain only when the

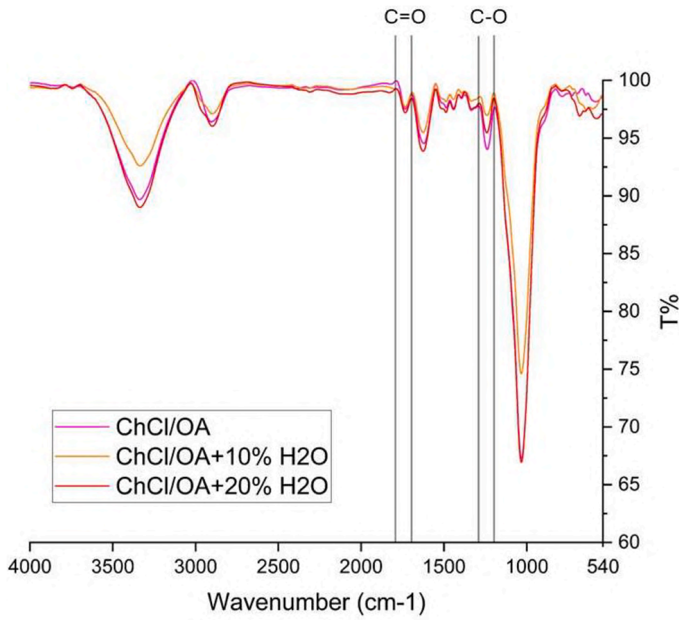

Fig. 7. FT-IR spectra of the SRs treated at 80 °C for 1 h with the ChCl/OA NADES without and with 10 % or 20 % water addition. The vertical grey lines mark the peaks due to esterification.

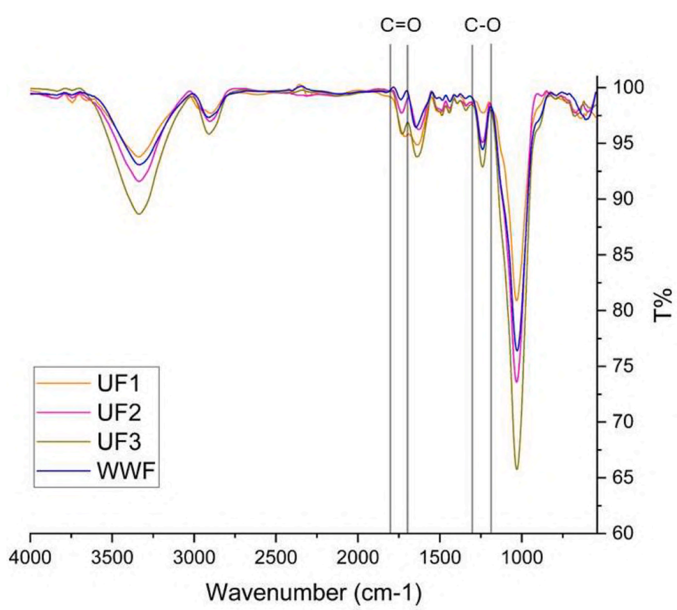

Fig. 8. FT-IR spectra of the SRs obtained from the ultrafast microwave reactions (UF1, UF2 and UF3) compared to the carpentry WWF. The vertical grey lines mark the wave number intervals indicative for esterification.

treated biomass is constituted by cellulose as the only component (Liu et al., 2021a). Herein, since the pristine biomass contained cellulose, hemicellulose and lignin, the IR analyses were not unambiguously clear, due to the overlapping of the possibly formed ester peaks with those of lignin, as shown in Figs. 6-8. In the present work, carboxylic acids used for DES mixtures had two (OA) or three (CA) carboxylic moieties. For this reason, after their esterification with the hydroxyl groups of cellulose (or hemicellulose), they should bring free carboxylic groups now directly connected to the resulting biomass. The carboxylic group content (CGC) in the solid residue (SR) after the treatment with various DES under different conditions was quantified using the titration method (Barbash et al., 2022). Table 2 summarizes the obtained results.

Table 2
carboxyl groups content (CGC) for each SR.

Entry	*Solid Residue*	*CGC [mmol/g]*
1	Cellulose	0.072
2	CWWF	0.115
3	SR from ChCl/OA	0.149
4	SR from ChCl/OA +10 %H_2O	0.190
5	SR from ChCl/OA +20 % H_2O	0.154
6	SR from ChCl/OA 90 °C	0.189
7	SR from ChCl/CA	0.157
8	SR from Betaine/OA	0.214
9	SR from ChCl/Urea	0.137
10	SR from UF1	0.190
11	SR from UF2	0.103
12	SR from UF3	0.131

Pure cellulose and the pristine CWWF were first titrated, giving negligible and small CGC values, respectively (entries 1 and 2, Table 2). Thus, CGC value of CWWF (0.115 mmol/g) could be taken as the zero initial point. In absolute terms, the amount of carboxyl groups was small for all SRs reported in Table 2. The highest CGC value (0.214 mmol/g, entry 8, Table 2) was reached in the case of Betaine/OA DES, which contained carboxylic groups in both hydrogen bond donor (HBD) and hydrogen bond acceptor (HBA) of the mixture. Moreover, SRs treated with ChCl/OA and ChCl/CA DES (entries 3 and 7 of Table 2) showed increasing CGC values due to the increasing number of carboxylic groups of the HBD unit. As to SR coming from the not-containing carboxylic groups ChCl/Urea DES (entry 9, Table 2), its CGC value (0.137 g/mmol) was slightly higher than that of CWWF probably due to the oxidation of some -OH groups in 7-position of the glucose monomers (Jiang & Hsieh, 2016). Interestingly, ChCl/OA treatments with 10 % H_2O addition at 80 °C (entry 4), without H_2O addition at 90 °C (entry 6) and under UF1 condition (entry 10) gave the same CGC values, while UF2 and UF3 seemed to promote negligible free acid esterification (entries 11 and 12), though IR analyses discussed in the previous paragraph suggested opposite consideration about SR coming from UF3.

3.1.4. Solid state ^{13}C NMR analyses

^{13}C CP/MAS NMR analyses are suitable to assess the crystallinity index (CrI) of the various SRs, which should change after DES treatment. In fact, since amorphous cellulose is more sensitive to hydrolysis than the crystalline one, its solubilization causes an increasing of CrI with respect to the starting lignocellulosic biomass (Yue et al., 2015). Table 3 reports CrI of the starting CWWF and those of the obtained SRs after DES treatment. CWWF has a CrI equal to 0.33, revealing that the amorphous phase was higher than the crystalline one in the pristine biomass. A slight increase of the crystalline phase over the amorphous phase was observed after all treatments. The highest values of CrI were detected for ChCl/OA SRs treated with 10 % H_2O addition (CrI = 0.40, entry 3) at 80 °C, without H_2O addition at 90 °C (CrI = 0.41, entry 5) and under UF1 condition (CrI = 0.45, entry 10), confirming the similarity of the three

Table 3
crystallinity indexes of the various SRs.

Entry	SR	Crystallinity Index
1	CWWF	0.33
2	SR from ChCl/OA	0.39
3	SR from ChCl/OA +10 %H2O	0.40
4	SR from ChCl/OA +20 %H2O	0.39
5	SR from ChCl/OA 90 °C	0.41
6	SR from ChCl/CA	0.35
7	SR from Betaine/OA	0.38
8	SR from ChCl/Urea	0.35
9	SR from K_2CO_3/Glycerol	0.36
10	SR from UF1	0.45
11	SR from UF2	0.36
12	SR from UF3	0.35

samples as already suggested by the analyses discussed in the previous paragraphs.

NMR analyses are also useful to qualitatively observe the possible disappearance of lignin-related peaks and/or the appearance of peaks related to the functionalisation of the residual solid with ester moieties (Vaidya et al., 2016). Fig. 9 shows ^{13}C CP/MAS NMR spectra of CWWF and SRs obtained after treatment with glycerol/K_2CO_3 and ChCl/OA, respectively, being the latter representative of the NMR spectra of all SRs reported in Table 1, except for entry 5. Signals associated to lignin, cellulose and hemicellulose were identified in the NMR spectrum of CWWF (Fig. 9a) and some of them decreased or even disappeared in the NMR spectra of SRs isolated after ChCl/OA and glycerol/K_2CO_3 treatment (Fig. 9b). The most intense signals in all spectra belonged to glucose units of cellulose and hemicellulose, allowing to distinguish between crystalline and amorphous phase in C4 and C6 resonance peaks, as already discussed. Lignin signals are visible in the aromatic regions (160÷110 ppm) as low intense and poorly resolved peaks. Lignin units coming from the three common monolignols (depicted in Figure S1) gave four broad bands at 158 ppm (carbon 4 of p-hydroxyphenyl units, H), 153 ppm (belonging to syringyl units, S), 148 ppm and 145 ppm (belonging to guaiacyl units, G) (Cipriano et al., 2020). All of them were visible in the ^{13}C CP/MAS NMR spectra of CWWF and SR treated with glycerol/K_2CO_3, and they became less intense in the ^{13}C CP/MAS NMR spectrum of SR treated with ChCl/OA, with the peak at 158 ppm being negligible (Fig. 9b). Another characteristic peak for lignin is the sharp signal at 56 ppm belonging to methoxy groups of S and G, which remained almost unchanged in all spectra, while the -CH_2 peak at 48 ppm (Kostryukov et al., 2021) detected in the spectra of CWWF and SR treated with glycerol/K_2CO_3 almost disappeared in the ^{13}C CP/MAS NMR spectrum of SR treated with ChCl/OA (Fig. 9b). The intensity of the signal at 20 ppm (Fig. 9a) related to the acetyl methyl moiety in hemicellulose (Figure S2) decreased on passing from CWWF spectrum to the ChCl/OA treated SR one, becoming almost negligible in the spectrum of SR isolated from glycerol/K_2CO_3 mixture (Fig. 9b). All these data indicate that ChCl/OA NADES selectively depolymerized a more amount of lignin than hemicellulose, while the alkaline glycerol/K_2CO_3 DES solubilized a more amount of hemicellulose than lignin, as already suggested by TGA analyses (Fig. 2).

3.1.5. Preliminary considerations after physical-chemical characterization

As highlighted by the analyses, CGC values of SRs suggested for the presence of carboxylic groups in the treated biomass that could potentially facilitate the mechanical disruption of the lignin-containing cellulose fibrils into nanoparticles. Indeed, the SRs still contain lignin, which is an aromatic and hydrophobic biopolymer, and can be useful in retaining organic pollutants by intermolecular interactions.

Thus, the features found in SRs obtained after DES treatments prompted us at testing them in two important fields: lignin-containing nanocellulose production and water decontamination from organic pollutants.

3.2. Producing lignin-rich nanocellulose

Valorisation of the solid residues obtained from lignocellulosic biomass treated with DES can be achieved with the synthesis of cellulose nanoparticles by means of mechanical disruption such as ball milling or ultrasonication (Jančíková & Jablonský, 2024; Wang et al., 2023). The yields of cellulose nanoparticles depend on several factors, such as biomass source, power of ultrasonication or speed of ball milling, pre-treatment conditions and so on (Tong et al., 2023). The biomass source dramatically affects the yield in nanocellulose, especially when the final product is a lignin-rich cellulose nanocrystal or nanofibril, being lignin structure very dependent on the kind of starting plant. In the present study, the starting CWWF biomass is a very heterogeneous substrate, and this feature could represent a disadvantage for finding the best conditions towards nanocellulose production with the ultrasonication method. Aiming at obtaining lignin-rich nanocellulose, all solid residues reported in Table 4 (column 2) were dispersed in water and subjected to ultrasonication in a common bath or with the use of a probe (as described in paragraph 2.4). The resulting cellulose derived nano-colloids were subjected to DLS measurements which assessed their size and stability in water suspension as well as the ζ-potential, the hydrodynamic diameter, and the polydispersity index. The yields in nanocellulose with respect to SRs were also calculated. All these data are summarized in Table 4. Nanocellulose yields were low ranging from 1.7 % to 13.7 % (Table 4), corresponding to 1.3 % and 9.2 %, respectively, if calculated on the starting feed raw material. Generally, under the same reaction conditions SRs coming from acidic DES (entries 1 and 6) gave higher yields than SRs from alkaline DES (entries 7 and 8), except for SR from ChCl/CA which furnished poor yield (entry 5). However, DES mixture based on ChCl/OA (entry 1) seemed to be the most capable material for producing nanocellulose, and the addition of water (entries 3 and 4) or the use of ultrafast conditions (entries 9 and 10) did not significantly affect the final yields. A significant increase in the final yield was observed when the ultrasonication probe (entry 2) was used in the place of the ultrasonication bath (entry 1), suggesting that the ultrasound conditions play a key role in the nanocellulose production.

Despite the poor yields, ζ-potential values ranged from −26 to −37 mV (Table 4) indicating a good colloidal stability of all samples. However, hydrodynamic diameter and polydispersity index values revealed that the ChCl/OA mixture provided the best colloidal suspension in terms of nano-size and mono-dispersity, respectively. In fact, with the ChCl/OA mixture the hydrodynamic diameter ranged from 223 to 303 nm (Entries 1–5, 9, 10, Table 4). Moreover, polydispersity index (PDI)

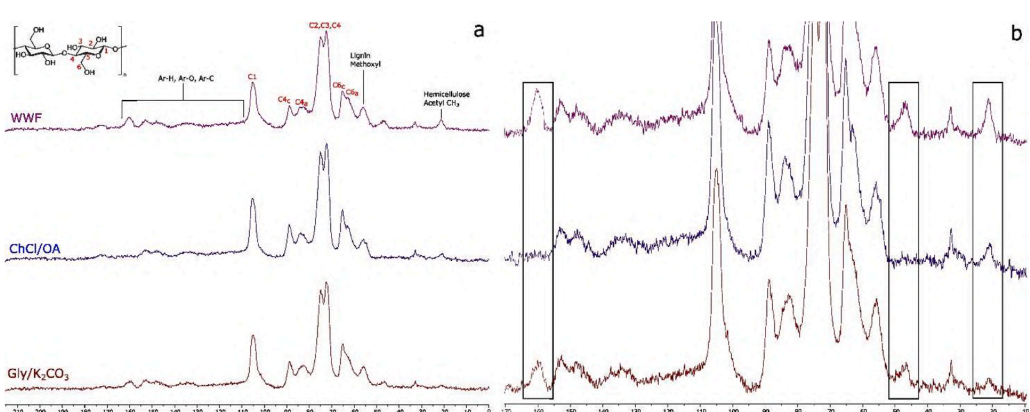

Fig. 9. a) Solid State ^{1}H-^{13}C– CP/MAS spectra of carpentry waste wood flour (in purple), solid residue obtained from the ChCl/OA treatment (in blue) and solid residue obtained from the Glycerol/K_2CO_3 treatment (in red); b) expanded region with marked sections.

Table 4
DLS parameters (ζ-potential, Average hydrodynamic diameter, PDI) measured on diluted samples in ultrapure water at the refractive index of cellulose (1.469) and nanocellulose yield percentage.

Entry	Solid Residues	Experimental conditions [a]	ζ-potential (mV) [b]	Average hydrodynamic diameter (nm) [c]	Polydispersity Index [d]	Nanocellulose Yield (%)
1	SR from ChCl/OA	Ultrasonication Bath	−37±2.4	223.3 ± 5.3	0.27±0.03	6.2
2	SR from ChCl/OA	Ultrasonication Probe	−26±0.25	268±8.5	0.37±0.01	13.7
3	SR from ChCl/OA +10 % H2O	Ultrasonication Bath	−32.5 ± 3.7	271±3.3	0.30±0.03	5.0
4	SR from ChCl/OA +20 % H2O	Ultrasonication Bath	−32.4 ± 2.8	303.5 ± 4	0.34±0.02	3.5
5	SR from ChCl/CA	Ultrasonication Bath	−27.3 ± 3.3	409±4.3	0.69±0.02	1.7
6	SR from Betaine/OA	Ultrasonication Bath	−28.5 ± 1.42	315±4.5	0.4 ± 0.02	5.8
7	SR from ChCl/Urea	Ultrasonication Bath	−30.5 ± 0.2	286±2.2	0.46±0.03	1.9
8	SR from K_2CO_3/Glycerol	Ultrasonication Bath	−33.2 ± 3.2	279±23.6	0.43±0.07	1.8
9	SR from UF2	Ultrasonication Bath	−29±1.3	301.4 ± 25	0.48±0.05	3.0
10	SR from UF3	Ultrasonication Bath	−32±2.5	269±8.4	0.45±0.08	7.3

[a] Experimental conditions for the ultrasonication process (bath or probe), as reported in paragraph 2.4.
[b] ζ-potential values are reported as the mean (±standard deviation) of 5 measurements; each of them derived from 20 different runs, to establish measurement repeatability; ζ-potential values ≥ ±20 mV indicate a stable colloidal suspension.
[c] Average hydrodynamic diameter is the Z-average (±standard deviation) of 3 Distribution Size measurements, each constituting of 14 runs; Z-average is the diameter of colloids in aqueous suspension and can also indicate the state of aggregation of the sample.
[d] Polydispersity Index (PDI) is reported as the mean (±standard deviation) of 3 Distribution Size measurements, each constituting of 14 runs; PDI value over 0.5 indicates polydisperse colloidal dispersion and not homogenous sample.

values indicated a moderately polydisperse distribution type only for nanoparticles generated from ChCl/OA SR (0.1<PDI<0.4, entries 1–4, Table 4), suggesting slightly broad distribution type for all other cases (PDI≥0.4, entries 5–10, Table 4). However, extremely broad distribution type (PDI>0.7) was never observed (Mudalige et al., 2019).

TEM analysis (Figs. 10-14) revealed that nanocellulose formed after all treatments was in the form of nanorods, nanosheets or nanospheres, as already observed for other lignocellulosic substrates treated with DESs (Pérez-Pérez et al., 2023; Smirnov et al., 2020; Wang et al., 2020a). Fig. 10 shows the TEM images of nanocellulose obtained by ultrasonication (ultrasonication bath) of SRs recovered after biomass treatment with ChCl/OA DES both in the absence and in the presence of water at different percentages.

Samples coming from ChCl/OA treatment were composed of both amorphous particles of almost spherical shape and diameter size in the range 200–500 nm, and crystalline nanorods with a thickness of about 40 nm and a length of over 500 nm (Fig. 10A-C). The addition of 10 % water to the ChCl/OA mixture caused the formation of more spherical, homogeneous particles with size ranging from 100 to 200 nm. However, they were amorphous, and no rods were detected (Fig. 10D-F). Samples coming from ChCl/OA/20 % H_2O treatment were made by thin nanofibers and very dark nanospheres of 10 nm which belonged to lignin nano-colloids (Liu et al., 2020) (Fig. 10G-I).

The process of ultrasonication by probe greatly improved the mono-

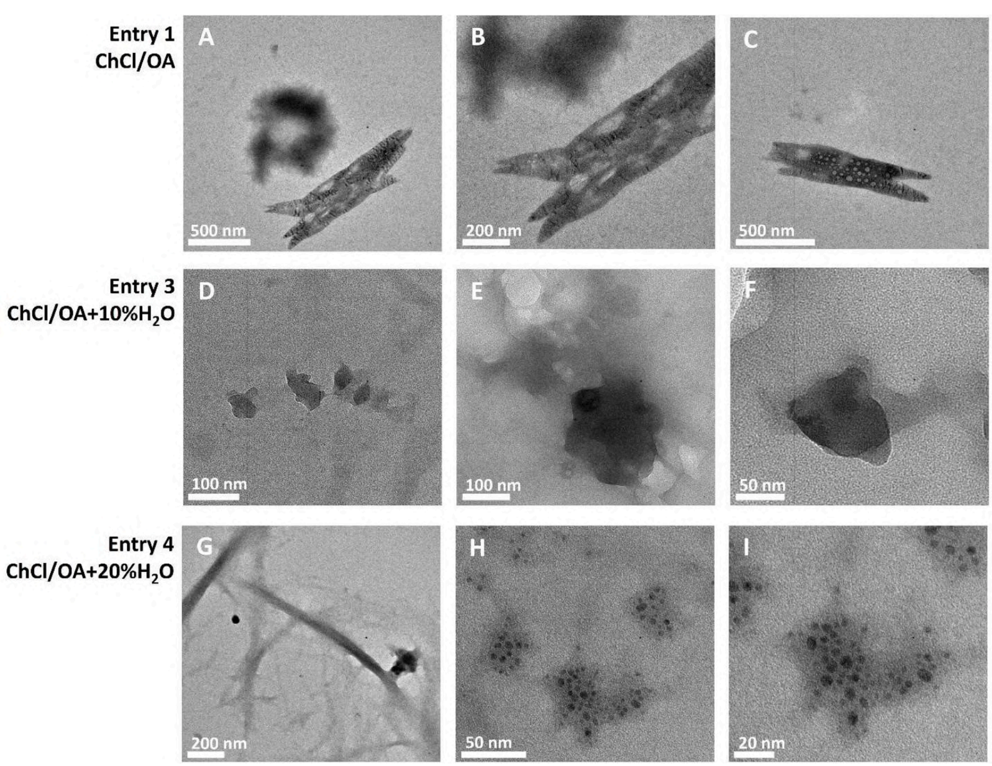

Fig. 10. TEM images of nanocellulose obtained by ultrasonication (bath) of SRs recovered after biomass treatment with: (**A, B,** C) ChCl/OA (Entry 1 of Table 4); (**D, E,** F) ChCl/OA/10 % H_2O (Entry 3 of Table 4); (**G, H,** I) ChCl/OA/20 % H_2O (Entry 4 of Table 4). The presence of water promoted lignin nano-colloids formation.

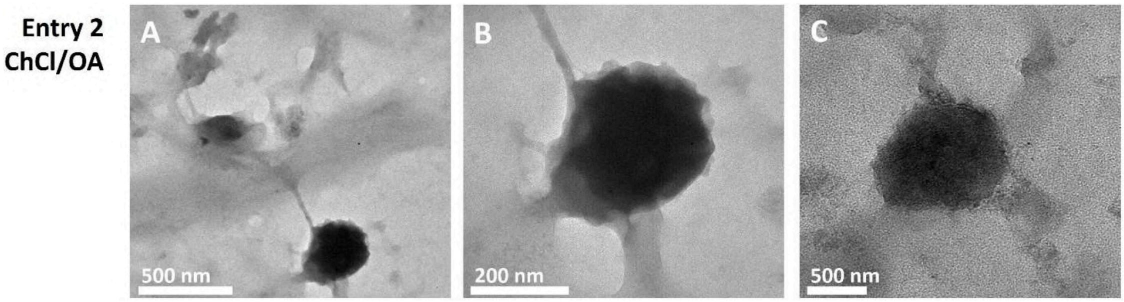

Fig. 11. nanocellulose obtained by ultrasonication (probe) of SR recovered after biomass treatment with ChCl/OA (Entry 2 of Table 4). The use of the ultrasonication probe (in the place of the ultrasonication bath) promoted the formation nanoparticles of spherical shape.

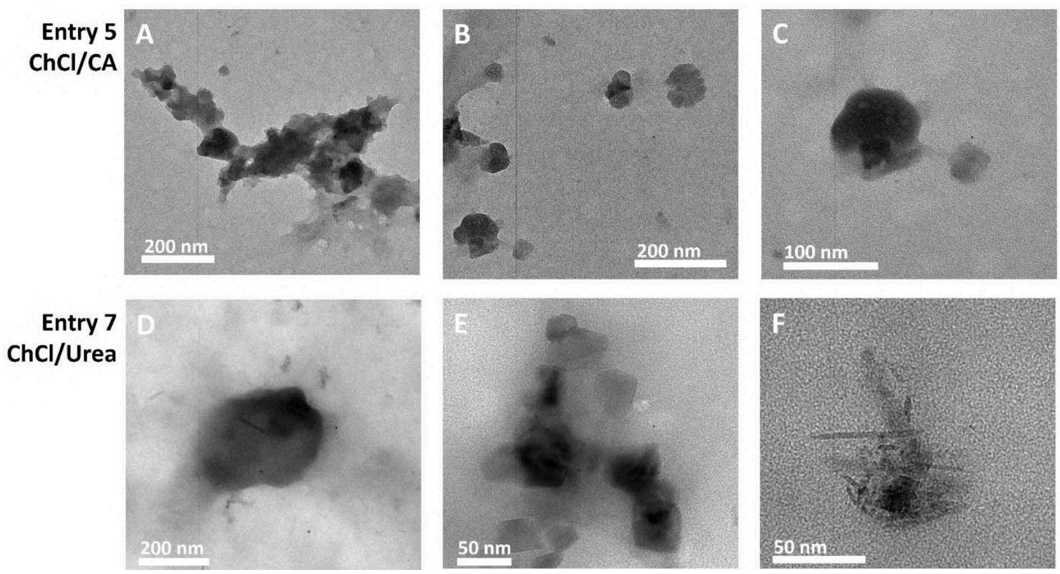

Fig. 12. TEM images of nanocellulose obtained by ultrasonication (bath) of SRs recovered after biomass treatment with: (**A, B,** C) ChCl/CA (Entry 5 of Table 4); (**D, E,** F) ChCl/urea (Entry 7 of Table 4) Nanocolloids with irregular shape were observed for both cases.

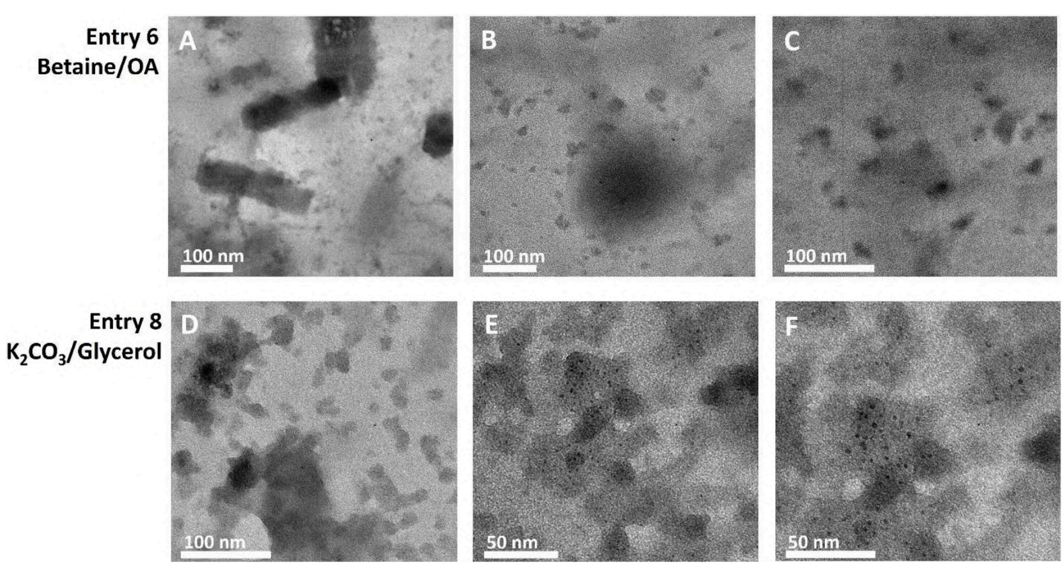

Fig. 13. TEM images of nanocellulose obtained by ultrasonication (bath) of SRs recovered after biomass treatment with: (**A, B,** C) Betaine/OA (Entry 6 of Table 4); (**D, E,** F) Glycerol/K_2CO_3 (Entry 8 of Table 4). A *core-shell* morphology was detected.

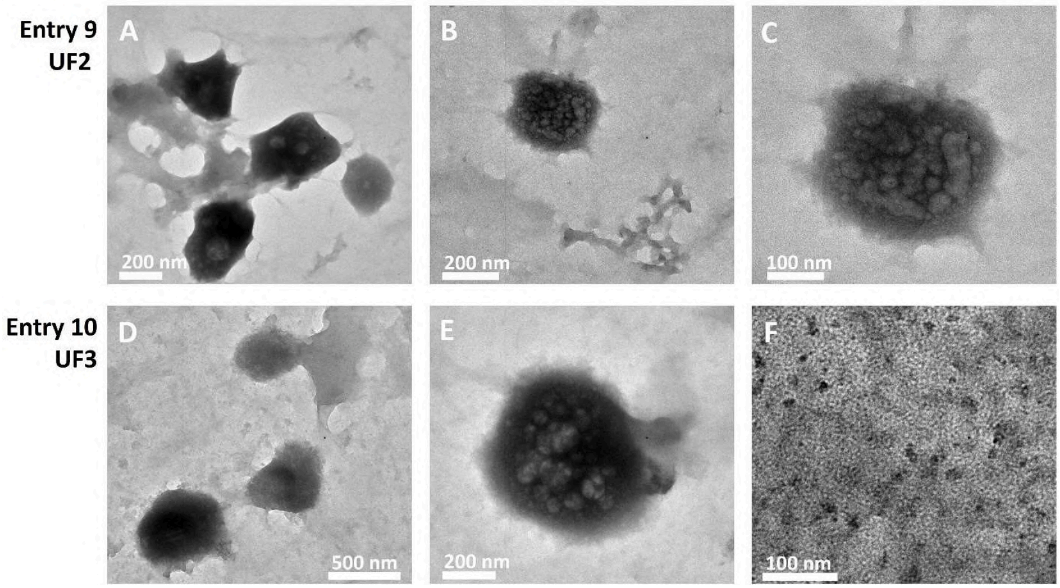

Fig. 14. TEM images of nanocellulose obtained by ultrasonication (bath) of SRs recovered after biomass treatment with ChCl/OA: (**A, B,** C) under UF2 conditions (Entry 9 of Table 4); (**D, E,** F) under UF3 conditions (Entry 10 of Table 4) A porous nature was observed.

dispersity of nanocellulose, and amorphous particles with a spherical shape and a diameter of around 200 nm were observed (Fig. 11).

The ChCl/CA mixture provided nanocolloids with irregular shape, assimilated to spheres, with a diameter of approximately 100 nm (Fig. 12A-C). The ChCl/Urea mixture formed larger particles than the previous treatments beside some nanocrystals (Fig. 12D-F).

Bath ultrasonication of SRs recovered after Betaine/OA and K_2CO_3/Glycerol biomass treatments produced cellulose nanoparticles with irregular shape (Fig. 13) characterized by a *core-shell* morphology, being the core presumably made by lignin, since TGA analyses revealed a big amount of lignin after DES dealings. Very thick rods were also observed (Fig. 13D).

TEM images of samples derived from UF 2 and UF 3 treatments showed the presence of nanoparticles with diameter size above 200 nm, with an interesting porous nature (Fig. 14A-E). Lignin nanoparticles were observed in UF 3 sample (Fig. 14F).

In summary, the use of the ultrasonication probe instead of a sonication bath greatly improved the final yield in nanoparticles by reducing the polydispersity nature of the colloids, thus producing a very homogeneous sample. However, the low yield of nanoparticles obtained was probably due to the heterogeneous nature of the biomass source.

3.3. Water decontamination: p-nitrophenol adsorption

Cellulose treated with DES has been reported to efficiently remove methylene blue from contaminated water due to its carboxylated surface (Cao et al., 2022). To check the water decontamination capability of the residual solids (SRs) recovered after MW-assisted DES treatment of carpentry waste wood flour, they were tested for the removal of the well-known environmental pollutant *p*-nitrophenol in water. This aromatic compound is largely used in industry for production of chemicals, pharmaceuticals, pesticides and dyes, and for leather tannery activities. Due to its presence in many industrial wastewaters and due to its high solubility in water, it can contaminate many water bodies (freshwater, ground water, marine environment, rivers, lakes and so on) and can potentially harm aquatic life, vegetables, and humans (Tiwari et al., 2019). Aiming at decontaminating from *p*-nitrophenol a model polluted water body, preliminary tests were carried out by mixing for 50 min 500 mg of each SR reported in Table 1 with 20 mL of a water solution containing 20 ppm of *p*-nitrophenol. The final amount of the pollutant in the water phase was measured by UV–Vis spectrophotometric analyses. The UV–Vis absorbance curves of the *p*-nitrophenol solution before and after its treatment with CWWF and all SRs are reported in Fig. 15.

Analysis of the UV–Vis absorbance spectra after 50 min showed that the starting waste material CWWF had its own capability of adsorption

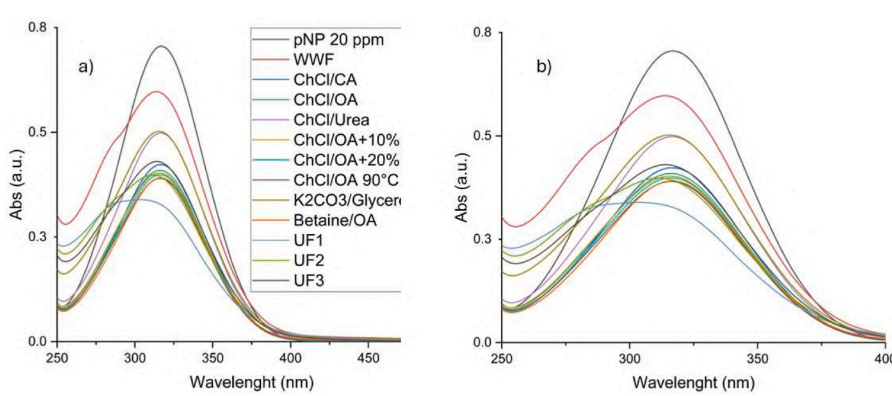

Fig. 15. a) UV–Vis absorbance spectra from 250 nm to 500 nm of the 20 ppm *p*-nitrophenol standard before and after the treatment with CWWF and the other SRs; b) expansion of the UV–Vis curves in the range 250–400 nm.

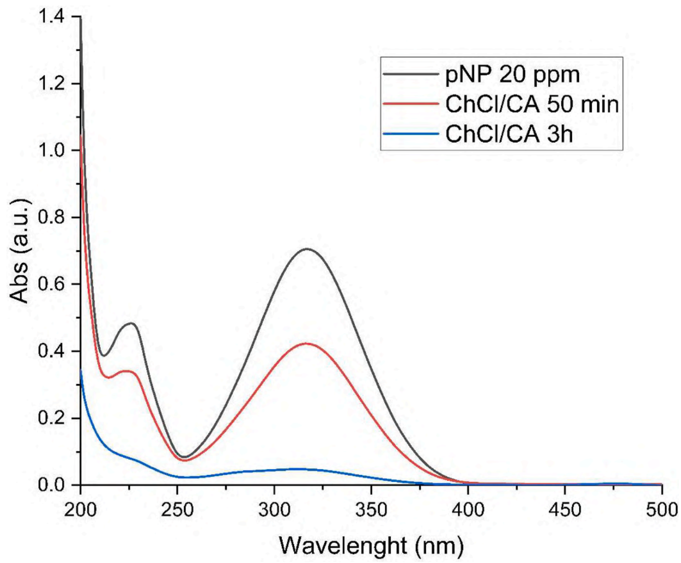

Fig. 16. UV–Vis absorbance spectra of the 20 ppm *p*-nitrophenol standard solution treated with ChCl/CA SR at *t*= 0 (grey line), after 50 min (red line) and after 3 h (blue line).

p-nitrophenol probably to hydrophobic π interactions between lignin and the aromatic ring of the contaminant. In fact, the maximum absorbance of the pollutant passed from 0.79 to 0.61 a.u. after mixing the standard water solution with CWWF for 50 min (Fig. 15b). All SRs had a higher capacity than CWWF to adsorb the aromatic contaminant. However, SRs treated with basic DES mixtures (glycerol/K_2CO_3 and betaine hydrochloride/OA) showed a lower degree of adsorption than SRs coming from acidic DES (Fig. 15b), probably due to the lower ability of alkaline DES of deconstructing the lignocellulosic biomass with respect to acidic DES. Since there were no significative differences among SRs coming from acidic DES in adsorbing the organic model pollutant, further studies were carried out by using the SR coming from ChCl/CA, because the latter gave the highest yield in solid residue (Entry 2 of Table 1). As depicted in Fig. 16, the amount of *p*-nitrophenol adsorbed by SR of ChCl/CA was almost 50 % after 50 min of contact time, becoming quantitative after 3 h mixing, demonstrating the efficiency of the treated lignocellulosic biomass as a sustainable sorbent for removing organic pollutants from water.

4. Conclusions

In the present work, carpentry waste wood flour (CWFF), which is a heterogeneous lignocellulosic biomass (70 % poplar and 30 % fir, *c.a.*), was subjected for the first time to microwave-assisted deep eutectic solvent treatment under different conditions and with several DES mixtures (acidic DESs, such as: ChCl/OA, ChCl/CA, Betaine hydrochloride/OA, and alkaline DESs, such as: Urea/ChCl, Glycerol/K_2CO_3). The resulting solid residues (SRs) were analysed by TGA, FT-IR, ^{13}C CP/MAS NMR spectroscopy. Crystallinity indexes, depolymerization yields and carboxylic group contents were also assessed. The following conclusions could be deduced about MW-assisted DES treatment of CWWF.

1) The best results in terms of *solubilization* of the starting lignocellulosic biomass were obtained with the acidic DES ChCl/OA and generally acidic DES depolymerized the initial material better than the alkaline ones.
2) With ChCl/OA DES treatment, the higher the temperature the higher the yield of *solubilization*, while the addition of 10 % H_2O to the ChCl/OA mixture slightly improved the *solubilization* yield, which is important in terms of atom economy and fluidity of the system.
3) After MW-assisted treatment with several DES mixtures, the resulting SRs contained cellulose, hemicellulose and lignin in relative amounts only depending on the used DES. The SRs coming from ChCl/OA under different conditions revealed a higher relative amount of cellulose compared to CWWF, while SR obtained from glycerol/K_2CO_3 DES showed an increased quantity of lignin with respect to pristine CWWF. In the other cases, the chemical compositions of the SRs were comparable to each other, revealing a substantial dissolution of hemicellulose.
4) IR and ^{13}C CP/MAS NMR were not suitable for quantifying the degree of esterification of alcoholic groups of SR carbohydrates with carboxylic acids of DES. On the contrary, the carboxylic group content (CGC) of SRs could be successfully determined by titration.
5) The highest values of carboxylic group content and crystallinity index were found in SRs treated with ChCl/OA either *i)* in the presence of 10 % H_2O at 80 °C (1 h under discontinuous MW irradiation), or *ii)* without H_2O addition at 90 °C (1 h under discontinuous MW irradiation), or *iii)* under UF1 condition (60 s at 156 °C under continuous MW irradiation), suggesting that the three procedures gave SRs with similar features.

Aiming at obtaining lignin-rich nanocellulose, all solid residues were dispersed in water and subjected to ultrasonication in a common bath or with the use of a probe. The resulting cellulose derived nano-colloids were evaluated by DLS measurements which assessed their size and stability in water suspension as well as the ζ-potential, the hydrodynamic diameter, and the polydispersity index. Nanocellulose yields were low ranging from 1.7 to 13.7 %, probably due to the heterogeneity of the starting material, since it is worldwide recognized that the LCB source highly affect the biorefinery outputs. However, despite the poor yields, ζ-potential values (from −26 to −37 mV) indicated a good colloidal stability of all samples. Moreover, hydrodynamic diameter and polydispersity index values revealed that the ChCl/OA mixture provided the best colloidal suspension in terms of nano-size and mono-dispersity.

On the base of the characterization results, all SRs seemed suitable for the adsorption of organic pollutants, due to the presence of pending esters and lignin, which should form hydrophobic interactions with organic compounds. Therefore, all SRs were tested for the adsorption of *p*-nitrophenol in water, taken as the model organic pollutant. Preliminary experiments showed that SRs treated with acidic DESs were able to retain the organic contaminant better than SRs recovered after treatment with alkaline DESs. Since among acidic DESs, ChCl/CA gave the highest yield in recovered SR (*i.e.* the lowest yield in depolymerization), only the latter was investigated in further experiments of water decontamination. The obtained results showed that SR coming from ChCl/CA was able to quantitively remove *p*-nitrophenol from a 20 ppm standard solution of the organic pollutant in water, opening new perspectives to DES-treatment of CWWF in the framework of environmental decontamination.

CRediT authorship contribution statement

Giovanni Cisternino: Writing – original draft, Methodology, Investigation, Formal analysis. **Francesca Baldassarre:** Formal analysis, Data curation. **Giuseppe Ciccarella:** Visualization, Formal analysis. **Piero Mastrorilli:** Writing – review & editing, Data curation. **Maria Michela Dell'Anna:** Writing – review & editing, Supervision, Funding acquisition, Data curation.

Declaration of competing interest

The authors declare that they have no known competing financial interests or personal relationships that could have appeared to influence the work reported in this paper.

Data availability

No data was used for the research described in the article.

Acknowledgments

POC PUGLIA FESR-FSE 2014/2020 "RIPARTI" is kindly acknowledged for financial support (fellowship). This work has been supported under the National Recovery and Resilience Plan (NRRP), Mission 4 Component 2 Investment 1.4 – Call for tender No 3138 of December 16, 2021 of the Italian Ministry of University and Research, funded by the European Union – NextGenerationEU [Award Number: CNMS named MOST, Concession Decree No 1033 of June 17, 2022, adopted by the Italian Ministery of University and Research, CUP: D93C22000410001, Spoke 14 "Hydrogen and New Fuels"]. Dr. Stefano Todisco is kindly acknowledged for recording all SSNMR spectra described herein.

Supplementary materials

Supplementary material associated with this article can be found, in the online version, at doi:10.1016/j.carpta.2024.100572.

References

Abbasi, A., Makhtoumi, Y., Wu, Y., & Chen, G. (2024). Characterization of cellulose nanocrystal extracted from household waste and its application for seed germination. *Carbohydrate Polymer Technologies and Applications, 7*, Article 100409. https://doi.org/10.1016/j.carpta.2023.100409

Abolore, R. S., Jaiswal, S., & Jaiswal, A. K. (2024). Green and sustainable pretreatment methods for cellulose extraction from lignocellulosic biomass and its applications: A review. In *Carbohydrate polymer technologies and applications, 7*. Elsevier Ltd. https://doi.org/10.1016/j.carpta.2023.100396

Ahmed, B., Gwon, J., Thapaliya, M., Adhikari, A., Ren, S., & Wu, Q. (2023). Combined effects of deep eutectic solvent and microwave energy treatments on cellulose fiber extraction from hemp bast. *Cellulose (London, England), 30*(5), 2895–2911. https://doi.org/10.1007/s10570-023-05081-3

Amesho, K. T. T., Lin, Y. C., Mohan, S. V., Halder, S., Ponnusamy, V. K., & Jhang, S. R. (2023). Deep eutectic solvents in the transformation of biomass into biofuels and fine chemicals: A review. In *Environmental chemistry letters, 21* pp. 183–230). Springer Science and Business Media Deutschland GmbH. https://doi.org/10.1007/s10311-022-01521-x

Amoroso, L., Muratore, G., Ortenzi, M. A., Gazzotti, S., Limbo, S., & Piergiovanni, L. (2020). Fast production of cellulose nanocrystals by hydrolytic-oxidative microwave-assisted treatment. *Polymers*, (1), 12. https://doi.org/10.3390/polym12010068

Baldassarre, F., Schiavi, D., Di Lorenzo, V., Biondo, F., Vergaro, V., Colangelo, G., Balestra, G. M., & Ciccarella, G. (2023). Cellulose nanocrystal-based emulsion of thyme essential oil: Preparation and characterisation as sustainable crop protection tool. *Molecules (Basel, Switzerland)*, (23), 28. https://doi.org/10.3390/molecules28237884

Barbash, V. A., Yashchenko, O. V., Gondovska, A. S., & Deykun, I. M. (2022). Preparation and characterization of nanocellulose obtained by TEMPO-mediated oxidation of organosolv pulp from reed stalks. *Applied Nanoscience (Switzerland), 12*(4), 835–848. https://doi.org/10.1007/s13204-021-01749-z

Bian, H., Chen, L., Dong, M., Fu, Y., Wang, R., Zhou, X., Wang, X., Xu, J., & Dai, H. (2020). Cleaner production of lignocellulosic nanofibrils: Potential of mixed enzymatic treatment. *Journal of Cleaner Production, 270*, Article 122506. https://doi.org/10.1016/j.jclepro.2020.122506

Boeriu, C. G., Bravo, D., Gosselink, R. J. A., & Van Dam, J. E. G. (2004). Characterisation of structure-dependent functional properties of lignin with infrared spectroscopy. *Industrial Crops and Products, 20*(2), 205–218. https://doi.org/10.1016/j.indcrop.2004.04.022

Calvo-Flores, F. G., & Mingorance-Sánchez, C. (2021). Deep eutectic solvents and multicomponent reactions: Two convergent items to green chemistry strategies. In *ChemistryOpen, 10* pp. 815–829). John Wiley and Sons Inc. https://doi.org/10.1002/open.202100137

Cao, X., Liu, M., Bi, W., Lin, J., & Chen, D. D. Y. (2022). Direct carboxylation of cellulose in deep eutectic solvent and its adsorption behavior of methylene blue. *Carbohydrate Polymer Technologies and Applications, 4*. https://doi.org/10.1016/j.carpta.2022.100222

Caputo, D., Fusco, C., Nacci, A., Palazzo, G., Murgia, S., D'Accolti, L., & Gentile, L. (2021). A selective cellulose/hemicellulose green solvents extraction from buckwheat chaff. *Carbohydrate Polymer Technologies and Applications, 2*(April), Article 100094. https://doi.org/10.1016/j.carpta.2021.100094

Ceaser, R., Rosa, S., Montané, D., Constantí, M., & Medina, F. (2023). Optimization of softwood pretreatment by microwave-assisted deep eutectic solvents at high solids loading. *Bioresource Technology, 369*. https://doi.org/10.1016/j.biortech.2022.128470. September 2022.

Channab, B. E., El Idrissi, A., Essamlali, Y., & Zahouily, M. (2024). Nanocellulose: Structure, modification, biodegradation and applications in agriculture as slow/controlled release fertilizer, superabsorbent, and crop protection: A review. *Journal of Environmental Management, 352*. https://doi.org/10.1016/j.jenvman.2023.119928

Chen, W., Yu, H., Liu, Y., Hai, Y., Zhang, M., & Chen, P. (2011). Isolation and characterization of cellulose nanofibers from four plant cellulose fibers using a chemical-ultrasonic process. *Cellulose (London, England), 18*(2), 433–442. https://doi.org/10.1007/s10570-011-9497-z

Chen, Z., & Wan, C. (2018). Ultrafast fractionation of lignocellulosic biomass by microwave-assisted deep eutectic solvent pretreatment. *Bioresource Technology, 250*, 532–537. https://doi.org/10.1016/j.biortech.2017.11.066. November 2017.

Chourasia, V. R., Pandey, A., Pant, K. K., & Henry, R. J. (2021). Improving enzymatic digestibility of sugarcane bagasse from different varieties of sugarcane using deep eutectic solvent pretreatment. *Bioresource Technology, 337*(July), Article 125480. https://doi.org/10.1016/j.biortech.2021.125480

Cipriano, D. F., Chinelatto, L. S., Nascimento, S. A., Rezende, C. A., de Menezes, S. M. C., & Freitas, J. C. C. (2020). Potential and limitations of 13C CP/MAS NMR spectroscopy to determine the lignin content of lignocellulosic feedstock. *Biomass and Bioenergy, 142*. https://doi.org/10.1016/j.biombioe.2020.105792

Colella, M., Romanazzi, G., Petrelli, V., Baldassarre, F., Ciccarella, G., Catauro, M., Mastrorilli, P., & Dell'Anna, M. M (2022). Microwave-assisted treatment of waste wood biomass with deep eutectic solvents. *Macromolecular Symposia, 404*(1), 2–5. https://doi.org/10.1002/masy.202100284

Coletti, A., Valerio, A., & Vismara, E. (2013). Posidonia oceanica as a renewable lignocellulosic biomass for the synthesis of cellulose acetate and glycidyl methacrylate grafted cellulose. *Materials, 6*(5), 2043–2058. https://doi.org/10.3390/ma6052043

Cui, Q., Peng, X., Yao, X. H., Wei, Z. F., Luo, M., Wang, W., Zhao, C. J., Fu, Y. J., & Zu, Y. G. (2015). Deep eutectic solvent-based microwave-assisted extraction of genistin, genistein and apigenin from pigeon pea roots. *Separation and Purification Technology, 150*, 63–72. https://doi.org/10.1016/j.seppur.2015.06.026

Duan, C., Tian, C., Feng, X., Tian, G., Liu, X., & Ni, Y. (2023). Ultrafast process of microwave-assisted deep eutectic solvent to improve properties of bamboo dissolving pulp. *Bioresource Technology, 370*(November 2022), Article 128543. https://doi.org/10.1016/j.biortech.2022.128543

Egorova, K. S., & Ananikov, V. P. (2014). Toxicity of ionic liquids: Eco(cyto)activity as complicated, but unavoidable parameter for task-specific optimization. *ChemSusChem, 7*(2), 336–360. https://doi.org/10.1002/cssc.201300459

Esposito, M. C., Corsi, I., Russo, G. L., Punta, C., Tosti, E., & Gallo, A. (2021). The era of nanomaterials: A safe solution or a risk for marine environmental pollution?. In *Biomolecules, 11* pp. 1–25) MDPI AG. https://doi.org/10.3390/biom11030441

Gan, P. G., Sam, S. T., Abdullah, M. F., Omar, M. F., & Tan, L. S. (2020). An alkaline deep eutectic solvent based on potassium carbonate and glycerol as pretreatment for the isolation of cellulose nanocrystals from empty fruit bunch. *Bioresources, 15*(1), 1154–1170. https://doi.org/10.15376/biores.15.1.1154-1170

Haldar, D., & Purkait, M. K. (2021). A review on the environment-friendly emerging techniques for pretreatment of lignocellulosic biomass: Mechanistic insight and advancements. In *Chemosphere, 264*. Elsevier Ltd. https://doi.org/10.1016/j.chemosphere.2020.128523

Hayyan, M., Abo-Hamad, A., AlSaadi, M. A. H., & Hashim, M. A. (2015). Functionalization of graphene using deep eutectic solvents. *Nanoscale Research Letters, 10*(1). https://doi.org/10.1186/s11671-015-1004-2

Nonappa Heise, K., Kontturi, E., Allahverdiyeva, Y., Tammelin, T., Linder, M. B., & Ikkala, O (2021). Nanocellulose: Recent fundamental advances and emerging biological and biomimicking applications. In *Advanced materials, 33*. Wiley-VCH Verlag. https://doi.org/10.1002/adma.202004349.

Hong, S., Yuan, Y., Li, P., Zhang, K., Lian, H., & Liimatainen, H. (2020). Enhancement of the nanofibrillation of birch cellulose pretreated with natural deep eutectic solvent. *Industrial Crops and Products, 154*(February), Article 112677. https://doi.org/10.1016/j.indcrop.2020.112677

Hou, Q., Ju, M., Li, W., Liu, L., Chen, Y., Yang, Q., & Zhao, H (2017). Pretreatment of lignocellulosic biomass with ionic liquids and ionic liquid-based solvent systems. In *Molecules, 22*. MDPI AG. https://doi.org/10.3390/molecules22030490

Isci, A., Erdem, G. M., Bagder Elmaci, S., Sakiyan, O., Lamp, A., & Kaltschmitt, M. (2020). Effect of microwave-assisted deep eutectic solvent pretreatment on lignocellulosic structure and bioconversion of wheat straw. *Cellulose (London, England), 27*(15), 8949–8962. https://doi.org/10.1007/s10570-020-03371-8

Jančíková, V., & Jablonský, M. (2024). Cellulose nanoproducts isolated from lignocellulosic materials using DES-like mixtures – A minireview: State-of-the-art 2023. *Journal of Molecular Liquids, 394*, Article 123645. https://doi.org/10.1016/J.MOLLIQ.2023.123645

Ji, Q., Yu, X., Yagoub, A. E. G. A., Chen, L., & Zhou, C. (2021). Efficient cleavage of strong hydrogen bonds in sugarcane bagasse by ternary acidic deep eutectic solvent and ultrasonication to facile fabrication of cellulose nanofibers. *Cellulose (London, England), 28*(10), 6159–6182. https://doi.org/10.1007/s10570-021-03876-w

Jiang, F., & Hsieh, Y. Lo (2016). Self-assembling of TEMPO oxidized cellulose nanofibrils as affected by protonation of surface carboxyls and drying methods. *ACS Sustainable Chemistry and Engineering, 4*(3), 1041–1049. https://doi.org/10.1021/acssuschemeng.5b01123

Kohli, K., Katuwal, S., Biswas, A., & Sharma, B. K. (2020). Effective delignification of lignocellulosic biomass by microwave assisted deep eutectic solvents. *Bioresource Technology, 303*. https://doi.org/10.1016/j.biortech.2020.122897

Kostryukov, S. G., Petrov, P. S., Kalyazin, V. A., Masterova, Y. Y., Tezikova, V. S., Khluchina, N. A., Labzina, L. Y., & Alalvan, D. K. (2021). Determination of lignin content in plant materials using solid-state 13C NMR spectroscopy. *Polymer Science - Series B, 63*(5), 544–552. https://doi.org/10.1134/S1560090421050067

Krasznai, D. J., Champagne Hartley, R., Roy, H. M., Champagne, P., & Cunningham, M. F (2018). Compositional analysis of lignocellulosic biomass: Conventional methodologies and future outlook. In *Critical reviews in biotechnology, 38* pp. 199–217). Taylor and Francis Ltd. https://doi.org/10.1080/07388551.2017.1331336

Kumar, A. K., & Sharma, S. (2017). Recent updates on different methods of pretreatment of lignocellulosic feedstocks: A review. In *Bioresources and bioprocessing, 4*. Springer Science and Business Media Deutschland GmbH. https://doi.org/10.1186/s40643-017-0137-9

Landge, V. K., Hakke, V. S., Kakunuri, M., Babu, G. U. B., Boczkaj, G., & Sonawane, S. H. (2022). Synthesis of bimetallic Co-Pt/cellulose nanocomposites for catalytic reduction of p -nitrophenol. *Reaction Chemistry and Engineering, 7*(3), 641–652. https://doi.org/10.1039/d1re00422k

Lee, M., Heo, M. H., Lee, H. H., Jeong, H., Kim, Y. W., & Shin, J. (2018). Facile and eco-friendly extraction of cellulose nanocrystals: Via electron beam irradiation followed by high-pressure homogenization. *Green Chemistry, 20*(11), 2596–2610. https://doi.org/10.1039/c8gc00577j

Li, P., Ma, H., Qian, S., Chen, Y., Lai, B., & Pu, S. (2023). Stabilization of nFeS with carboxymethyl cellulose for enhancing persulfate activation for p-Nitrophenol degradation. *Journal of Environmental Chemical Engineering, 11*(2). https://doi.org/10.1016/j.jece.2023.109272

Lin, W., Xing, S., Jin, Y., Lu, X., Huang, C., & Yong, Q. (2020). Insight into understanding the performance of deep eutectic solvent pretreatment on improving enzymatic digestibility of bamboo residues. *Bioresource Technology, 306*(February), Article 123163. https://doi.org/10.1016/j.biortech.2020.123163

Liu, C., Li, M. C., Chen, W., Huang, R., Hong, S., Wu, Q., & Mei, C. (2020). Production of lignin-containing cellulose nanofibers using deep eutectic solvents for UV-absorbing polymer reinforcement. *Carbohydrate Polymers*, 246. https://doi.org/10.1016/j.carbpol.2020.116548

Liu, E., Meng, H., Zhang, H., Liang, H., & Wu, Z. (2023). Nanocellulose, a renewable biobased Functional/Reinforcement additive for composite coating materials: A review. *ACS Applied Polymer Materials*. https://doi.org/10.1021/acsapm.3c02088

Liu, Q., Yuan, T., Fu, Q.jin, Bai, Y.yuan, Peng, F., & Yao, C.li (2019). Choline chloride-lactic acid deep eutectic solvent for delignification and nanocellulose production of moso bamboo. *Cellulose (London, England), 26*(18), 9447–9462. https://doi.org/10.1007/s10570-019-02726-0

Liu, S., Zhang, Q., Gou, S., Zhang, L., & Wang, Z. (2021a). Esterification of cellulose using carboxylic acid-based deep eutectic solvents to produce high-yield cellulose nanofibers. *Carbohydrate Polymers, 251*, Article 117018. https://doi.org/10.1016/j.carbpol.2020.117018. August 2020.

Liu, W., Du, H., Liu, K., Liu, H., Xie, H., Si, C., Pang, B., & Zhang, X. (2021b). Sustainable preparation of cellulose nanofibrils via choline chloride-citric acid deep eutectic solvent pretreatment combined with high-pressure homogenization. *Carbohydrate Polymers, 267*(April), Article 118220. https://doi.org/10.1016/j.carbpol.2021.118220

Liu, W., Jiang, C., Li, X., Li, H., Zhang, Y., Huang, Y., Chen, S., & Hou, Q. (2024). Microwave-assisted DES fabrication of lignin-containing cellulose nanofibrils and its derived composite conductive hydrogel. *Carbohydrate Polymers, 328*, Article 121741. https://doi.org/10.1016/j.carbpol.2023.121741

Liu, Y., Chen, W., Xia, Q., Guo, B., Wang, Q., Liu, S., Liu, Y., Li, J., & Yu, H. (2017a). Efficient cleavage of lignin–carbohydrate complexes and ultrafast extraction of lignin oligomers from wood biomass by microwave-assisted treatment with deep eutectic solvent. *ChemSusChem, 10*(8), 1692–1700. https://doi.org/10.1002/cssc.201601795

Liu, Y., Guo, B., Xia, Q., Meng, J., Chen, W., Liu, S., Wang, Q., Liu, Y., Li, J., & Yu, H. (2017b). Efficient cleavage of strong hydrogen bonds in cotton by deep eutectic solvents and facile fabrication of cellulose nanocrystals in high yields. *ACS Sustainable Chemistry and Engineering, 5*(9), 7623–7631. https://doi.org/10.1021/acssuschemeng.7b00954

Lombardo, S., & Thielemans, W. (2019). Thermodynamics of adsorption on nanocellulose surfaces. In *Cellulose, 26* pp. 249–279). Springer Netherlands. https://doi.org/10.1007/s10570-018-02239-2

Ma, C., Svärd, M., & Forsberg, K. (2022). Recycling cathode material LiCo1/3Ni1/3Mn1/3O2 by leaching with a deep eutectic solvent and metal recovery with antisolvent crystallization. *Resources, Conservation and Recycling*, (August), 186. https://doi.org/10.1016/j.resconrec.2022.106579

Ma, Y., Xia, Q., Liu, Y., Chen, W., Liu, S., Wang, Q., Liu, Y., Li, J., & Yu, H. (2019). Production of nanocellulose using hydrated deep eutectic solvent combined with ultrasonic treatment [Research-article]. *ACS Omega, 4*(5), 8539–8547. https://doi.org/10.1021/acsomega.9b00519

Mahfoudhi, N., & Boufi, S. (2017). Nanocellulose as a novel nanostructured adsorbent for environmental remediation: A review. In *Cellulose, 24* pp. 1171–1197). Springer Netherlands. https://doi.org/10.1007/s10570-017-1194-0

Mankar, A. R., Pandey, A., & Pant, K. K. (2022). Microwave-assisted extraction of lignin from coconut coir using deep eutectic solvents and its valorization to aromatics. *Bioresource Technology, 345*, Article 126528. https://doi.org/10.1016/j.biortech.2021.126528. October 2021.

Martelli-Tosi, M., Masson, M. M., Silva, N. C., Esposto, B. S., Barros, T. T., Assis, O. B. G., & Tapia-Blácido, D. R. (2018). Soybean straw nanocellulose produced by enzymatic or acid treatment as a reinforcing filler in soy protein isolate films. *Carbohydrate Polymers, 198*(June), 61–68. https://doi.org/10.1016/j.carbpol.2018.06.053

Mjalli, F. S., Naser, J., Jibril, B., Al-Hatmi, S. S., & Gano, Z. S. (2014). Ionic liquids analogues based on potassium carbonate. *Thermochimica Acta, 575*, 135–143. https://doi.org/10.1016/j.tca.2013.10.028

Mudalige, T., Qu, H., Van Aute, D., Ansar, S. M., Paredes, A., & Ingle, T. (2019). Chapter 11 – Characterization of nanomaterials: Tools and challenges. *Micro and nano technologies, nanomaterials for food application* (pp. 313–353). Elsevier. https://doi.org/10.1016/B978-0-12-814130-4.00011-7

Nam, M. W., Zhao, J., Lee, M. S., Jeong, J. H., & Lee, J. (2015). Enhanced extraction of bioactive natural products using tailor-made deep eutectic solvents: Application to flavonoid extraction from Flos sophorae. *Green Chemistry, 17*(3), 1718–1727. https://doi.org/10.1039/c4gc01556h

New, E. K., Tnah, S. K., Voon, K. S., Yong, K. J., Procentese, A., Yee Shak, K. P., Subramonian, W., Cheng, C. K., & Wu, T. Y (2022). The application of green solvent in a biorefinery using lignocellulosic biomass as a feedstock. *Journal of Environmental Management, 307*. https://doi.org/10.1016/j.jenvman.2021.114385

Oh, Y., Park, S., Jung, D., Oh, K. K., & Lee, S. H. (2020). Effect of hydrogen bond donor on the choline chloride-based deep eutectic solvent-mediated extraction of lignin from pine wood. *International Journal of Biological Macromolecules, 165*, 187–197. https://doi.org/10.1016/j.ijbiomac.2020.09.145

Okonkwo, C. E., Hussain, S. Z., Manzoor, S., Naseer, B., Taiwo, A. E., Ayyash, M., Al-Marzouqi, A. H., & Kamal-Eldin, A. (2023). A comprehensive review on the use of deep eutectic solvents for biomass processing, and the synergistic coupling with physical technology and biological method. *Bioresource Technology Reports, 23*, Article 101577. https://doi.org/10.1016/J.BITEB.2023.101577

Patel, D. K., Dutta, S. D., & Lim, K. T. (2019). Nanocellulose-based polymer hybrids and their emerging applications in biomedical engineering and water purification. In *RSC advances, 9* pp. 19143–19162). Royal Society of Chemistry. https://doi.org/10.1039/c9ra03261d

Pérez-Pérez, A., Del-Río, P. G., Lobato-Rodríguez, Á., Garrote, G., & Gullón, B. (2023). Synergetic effect of hydrothermal and deep eutectic solvents (DES) pretreatments on Robinia wood fractionation for the manufacture of bioethanol and cellulose nanocrystals. *Industrial Crops and Products, 203*. https://doi.org/10.1016/j.indcrop.2023.117157

Pradhan, D., Jaiswal, A. K., & Jaiswal, S. (2022). Emerging technologies for the production of nanocellulose from lignocellulosic biomass. *Carbohydrate Polymers, 285*(February), Article 119258. https://doi.org/10.1016/j.carbpol.2022.119258

Prado, R., Erdocia, X., & Labidi, J. (2013). Lignin extraction and purification with ionic liquids. *Journal of Chemical Technology and Biotechnology, 88*(7), 1248–1257. https://doi.org/10.1002/jctb.3965

Rojo, E., Peresin, M. S., Sampson, W. W., Hoeger, I. C., Vartiainen, J., Laine, J., & Rojas, O. J. (2015). Comprehensive elucidation of the effect of residual lignin on the physical, barrier, mechanical and surface properties of nanocellulose films. *Green Chemistry, 17*(3), 1853–1866. https://doi.org/10.1039/c4gc02398f

Shao, H., He, L., Xiang, L., Tang, K., Li, X., Qi, J., & Xie, J. (2021). Transparent and UV-absorbing nanocellulose films prepared by directly dissolving microwave liquefied bamboo in TBAA/DMSO co-solvent system. *Industrial Crops and Products, 171*. https://doi.org/10.1016/j.indcrop.2021.113899

Siani, G., Tiecco, M., Di Profio, P., Guernelli, S., Fontana, A., Ciulla, M., & Canale, V. (2020). Physical absorption of CO2 in betaine/carboxylic acid-based natural deep eutectic solvents. *Journal of Molecular Liquids, 315*, Article 113708. https://doi.org/10.1016/j.molliq.2020.113708

Sirviö, J. A., Visanko, M., & Liimatainen, H. (2015). Deep eutectic solvent system based on choline chloride-urea as a pre-treatment for nanofibrillation of wood cellulose. *Green Chemistry, 17*(6), 3401–3406. https://doi.org/10.1039/c5gc00398a

Sirviö, J. A., Visanko, M., & Liimatainen, H. (2016). Acidic deep eutectic solvents as hydrolytic media for cellulose nanocrystal production. *Biomacromolecules, 17*(9), 3025–3032. https://doi.org/10.1021/acs.biomac.6b00910

Smirnov, M. A., Sokolova, M. P., Tolmachev, D. A., Vorobiov, V. K., Kasatkin, I. A., Smirnov, N. N., Klaving, A. V., Bobrova, N. V., Lukasheva, N. V., & Yakimansky, A. V. (2020). Green method for preparation of cellulose nanocrystals using deep eutectic solvent. *Cellulose (London, England), 27*(8), 4305–4317. https://doi.org/10.1007/s10570-020-03100-1

Smith, E. L., Abbott, A. P., & Ryder, K. S. (2014). Deep eutectic solvents (DESs) and their applications. In *Chemical reviews, 114* pp. 11060–11082). American Chemical Society. https://doi.org/10.1021/cr300162p

Tang, X., Zuo, M., Li, Z., Liu, H., Xiong, C., Zeng, X., Sun, Y., Hu, L., Liu, S., Lei, T., & Lin, L. (2017). Green processing of lignocellulosic biomass and its derivatives in deep eutectic solvents. In *ChemSusChem, 10* pp. 2696–2706). Wiley-VCH Verlag. https://doi.org/10.1002/cssc.201700457

Tiwari, J., Tarale, P., Sivanesan, S., & Bafana, A. (2019). Environmental persistence, hazard, and mitigation challenges of nitroaromatic compounds. In *Environmental science and pollution research, 26* pp. 28650–28667). Springer Verlag. https://doi.org/10.1007/s11356-019-06043-8

Tong, J., Hu, W., Qin, Y., & Liu, Y. (2023). Deep eutectic solvent pretreatment for green preparation of nanocellulose. In *Cellulose, 30* pp. 4773–4792). Springer Science and Business Media B.V. https://doi.org/10.1007/s10570-023-05154-3

Ünlü, A. E., Arlkaya, A., & Takaç, S. (2019). Use of deep eutectic solvents as catalyst: A mini-review. *Green Processing and Synthesis, 8*(1), 355–372. https://doi.org/10.1515/gps-2019-0003

Vaidya, A. A., Gaugler, M., & Smith, D. A. (2016). Green route to modification of wood waste, cellulose and hemicellulose using reactive extrusion. *Carbohydrate Polymers, 136*, 1238–1250. https://doi.org/10.1016/j.carbpol.2015.10.033

Verdía Barbará, P., Abouelela Rafat, A., Hallett, J. P., & Brandt-Talbot, A. (2023). Purifying cellulose from major waste streams using ionic liquids and deep eutectic solvents. In *Current opinion in green and sustainable chemistry, 41*. Elsevier B.V. https://doi.org/10.1016/j.cogsc.2023.100783

Vu, H. P., Nguyen, L. N., Vu, M. T., Johir, M. A. H., McLaughlan, R., & Nghiem, L. D. (2020). A comprehensive review on the framework to valorise lignocellulosic biomass as biorefinery feedstocks. *Science of the Total Environment, 743*. https://doi.org/10.1016/j.scitotenv.2020.140630

Wang, D. (2019). A critical review of cellulose-based nanomaterials for water purification in industrial processes. In *Cellulose, 26* pp. 687–701). Springer Netherlands. https://doi.org/10.1007/s10570-018-2143-2

Wang, H., Li, J., Zeng, X., Tang, X., Sun, Y., Lei, T., & Lin, L. (2020a). Extraction of cellulose nanocrystals using a recyclable deep eutectic solvent. *Cellulose (London, England), 27*(3), 1301–1314. https://doi.org/10.1007/s10570-019-02867-2

Wang, J., Jing, W., Tian, H., Liu, M., Yan, H., Bi, W., & Chen, D. D. Y. (2020b). Investigation of deep eutectic solvent-based microwave-assisted extraction and efficient recovery of natural products. *ACS Sustainable Chemistry and Engineering, 8* (32), 12080–12088. https://doi.org/10.1021/acssuschemeng.0c03393

Wang, J., Xu, J., Zhu, S., Wu, Q., Li, J., Gao, Y., Wang, B., Li, J., Gao, W., Zeng, J., & Chen, K. (2021). Preparation of nanocellulose in high yield via chemi-mechanical synergy. *Carbohydrate Polymers, 251*(July 2020), Article 117094. https://doi.org/10.1016/j.carbpol.2020.117094

Wang, X., Guo, J., Ren, H., Jin, J., He, H., Jin, P., Wu, Z., & Zheng, Y. (2024). Research progress of nanocellulose-based food packaging. In *Trends in food science and technology, 143*. Elsevier Ltd. https://doi.org/10.1016/j.tifs.2023.104289

Wang, Y., Liu, H., Ji, X., Wang, Q., Tian, Z., & Fatehi, P. (2023). Production of nanocellulose using acidic deep eutectic solvents based on choline chloride and carboxylic acids: A review. *International Journal of Biological Macromolecules, 245*. https://doi.org/10.1016/j.ijbiomac.2023.125227

Wu, M., Pang, J., Zhang, X., & Sun, R. (2014). Enhancement of lignin biopolymer isolation from hybrid poplar by organosolv pretreatments. *International Journal of Polymer Science*. https://doi.org/10.1155/2014/194726. *2014*.

Xiao, T., Hou, M., Guo, X., Cao, X., Li, C., Zhang, Q., Jia, W., Sun, Y., Guo, Y., & Shi, H. (2024). Recent progress in deep eutectic solvent(DES) fractionation of lignocellulosic components: A review. In *Renewable and sustainable energy reviews, 192*. Elsevier Ltd. https://doi.org/10.1016/j.rser.2023.114243

Xie, J., Hse, C. Y., De Hoop, C. F., Hu, T., Qi, J., & Shupe, T. F. (2016). Isolation and characterization of cellulose nanofibers from bamboo using microwave liquefaction combined with chemical treatment and ultrasonication. *Carbohydrate Polymers, 151*, 725–734. https://doi.org/10.1016/j.carbpol.2016.06.011

Yaneva, Z. L., Koumanova, B. K., & Allen, S. J. (2013). Applicability comparison of different kinetic/diffusion models for 4-nitrophenol sorption on Rhizopus oryzae dead biomass. *Bulgarian Chemical Communications, 45*(2).

Yu, W., Wang, C., Yi, Y., Zhou, W., Wang, H., Yang, Y., & Tan, Z. (2019). Choline chloride-based deep eutectic solvent systems as a pretreatment for nanofibrillation of ramie fibers. *Cellulose (London, England), 26*(5), 3069–3082. https://doi.org/10.1007/s10570-019-02290-7

Yue, Y., Han, J., Han, G., Zhang, Q., French, A. D., & Wu, Q. (2015). Characterization of cellulose I/II hybrid fibers isolated from energycane bagasse during the delignification process: Morphology, crystallinity and percentage estimation. *Carbohydrate Polymers, 133*, 438–447. https://doi.org/10.1016/j.carbpol.2015.07.058

Zainal-Abidin, M. H., Hayyan, M., Ngoh, G. C., Wong, W. F., & Looi, C. Y. (2019). Emerging frontiers of deep eutectic solvents in drug discovery and drug delivery systems. *Journal of Controlled Release, 316*(September), 168–195. https://doi.org/10.1016/j.jconrel.2019.09.019

Zhang, L., Tsuzuki, T., & Wang, X. (2015). Preparation of cellulose nanofiber from softwood pulp by ball milling. *Cellulose (London, England), 22*(3), 1729–1741. https://doi.org/10.1007/s10570-015-0582-6

Zhang, Y., & Naebe, M. (2021). Lignin: A review on structure, properties, and applications as a light-colored UV absorber. In *ACS sustainable chemistry and engineering, 9* pp. 1427–1442). American Chemical Society. https://doi.org/10.1021/acssuschemeng.0c06998

Zhou, C., Wu, Q., Lei, T., & Negulescu, I. I. (2014). Adsorption kinetic and equilibrium studies for methylene blue dye by partially hydrolyzed polyacrylamide/cellulose nanocrystal nanocomposite hydrogels. *Chemical Engineering Journal, 251*, 17–24. https://doi.org/10.1016/j.cej.2014.04.034

Zhou, M., Lv, M., Cai, S., & Tian, X. (2023). Effects of enzymatic hydrolysis and physicochemical properties of lignocellulose waste through different choline based deep eutectic solvents (DESs) pretreatment. *Industrial Crops and Products, 195*, Article 116435. https://doi.org/10.1016/J.INDCROP.2023.116435